

UNCLASSIFIED

AD NUMBER
ADB011796
NEW LIMITATION CHANGE
TO Approved for public release, distribution unlimited
FROM Distribution authorized to U.S. Gov't. agencies and their contractors; Administrative/Operational Use; Jul 1975. Other requests shall be referred to Air Force Wright Aeronautical Laboratories, Wright-Patterson AFB, OH 45433.
AUTHORITY
AFAL ltr, 16 Nov 1978

THIS PAGE IS UNCLASSIFIED

A46

AFML-TR-75-130
ADB011796

OFFICIAL FILE COPY

**THERMOGRAVIMETRIC-MASS
SPECTROMETRIC POLYMER
ANALYSIS**

*RESEARCH APPLICATIONS DIVISION
SYSTEMS RESEARCH LABORATORIES, INC.
2800 INDIAN RIPPLE ROAD
DAYTON, OHIO 45440*

JULY 1975

TECHNICAL REPORT AFML-TR-75-130
REPORT FOR PERIOD APRIL 1974 - MARCH 1975

Distribution limited to U.S. Government agencies only; (test and evaluation). June 1975. Other requests for this document must be referred to the Air Force Materials Laboratory, Nonmetallic Materials Division, Polymer Branch, AFML/MBP, Wright-Patterson Air Force Base, Ohio 45433.

AIR FORCE MATERIALS LABORATORY
AIR FORCE WRIGHT AERONAUTICAL LABORATORIES
Air Force Systems Command
Wright-Patterson Air Force Base, Ohio 45433

Best Available Copy

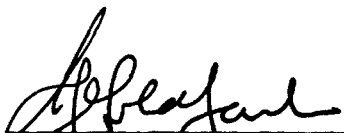
20040301128

OFFICIAL FILE COPY


NOTICE

When Government drawings, specifications or other data are used for any purpose other than in connection with a definitely related Government procurement operation, the United States Government thereby incurs no responsibility nor any obligation whatsoever; and the fact that the Government may have formulated, furnished, or in any way supplied the said drawings, specifications, or other data, is not to be regarded by implication or otherwise as in any manner licensing the holder or any other person or corporation, or conveying any rights or permission to manufacture, use, or sell any patented invention that may in any way be related thereto.

This technical report has been reviewed and is approved for publication.


I. J. GOLDFARB
Project Monitor

FOR THE COMMANDER


R. L. VAN DEUSEN, Chief
Polymer Branch
Nonmetallic Materials Division

Copies of this report should not be returned unless return is required by security considerations, contractual obligations, or notice on a specific document.

UNCLASSIFIED

SECURITY CLASSIFICATION OF THIS PAGE (When Data Entered)

REPORT DOCUMENTATION PAGE		READ INSTRUCTIONS BEFORE COMPLETING FORM
1. REPORT NUMBER AFML-TR-75-130	2. GOVT ACCESSION NO.	3. RECIPIENT'S CATALOG NUMBER
4. TITLE (and Subtitle) THERMOGRAVIMETRIC-MASS SPECTROMETRIC POLYMER ANALYSIS		5. TYPE OF REPORT & PERIOD COVERED Technical April 1974 - March 1975
		6. PERFORMING ORG. REPORT NUMBER
7. AUTHOR(s) E. G. Jones and P. A. Benadum		8. CONTRACT OR GRANT NUMBER(s) F33615-72-C-1537
9. PERFORMING ORGANIZATION NAME AND ADDRESS Systems Research Laboratories, Inc. 2800 Indian Ripple Road Dayton, Ohio 45440		10. PROGRAM ELEMENT, PROJECT, TASK AREA & WORK UNIT NUMBERS 7340-04-50
11. CONTROLLING OFFICE NAME AND ADDRESS Air Force Materials Laboratory Air Force Wright Aeronautical Laboratories Air Force Systems Command Wright Patterson Air Force Base, Ohio 45433		12. REPORT DATE July 1975
		13. NUMBER OF PAGES 88
14. MONITORING AGENCY NAME & ADDRESS (if different from Controlling Office)		15. SECURITY CLASS. (of this report) UNCLASSIFIED
		15a. DECLASSIFICATION/DOWNGRADING SCHEDULE
16. DISTRIBUTION STATEMENT (of this Report) Distribution limited to U.S. Government agencies only; (test and evaluation). June 1975. Other requests for this document must be referred to the Air Force Materials Laboratory, Nonmetallic Materials Division, Polymer Branch, AFML/MBP, Wright-Patterson AFB, Ohio 45433.		
17. DISTRIBUTION STATEMENT (of the abstract entered in Block 20, if different from Report)		
18. SUPPLEMENTARY NOTES		
19. KEY WORDS (Continue on reverse side if necessary and identify by block number) Polymer Analysis Mass Spectra Polymer Degradation Thermogravimetry		
20. ABSTRACT (Continue on reverse side if necessary and identify by block number) Thermogravimetric-mass spectral (TGMS) analyses of the volatile products of thermal degradation of sixteen polymers are reported. Perfluoro- and perfluoroether-substituted benzoxazoles comprise the majority of the samples. Perfluoro-substituted benzoxazoles, in general, display one temperature region of volatile-product formation. The volatile products tend to be perfluorocarbons. Perfluoroether-substituted benzoxazoles, depending upon the structure and loca- tion of the substitution, tend to display one or two temperature regions of		

DD FORM 1 JAN 73 1473

EDITION OF 1 NOV 65 IS OBSOLETE

UNCLASSIFIED

SECURITY CLASSIFICATION OF THIS PAGE (When Data Entered)

UNCLASSIFIED

SECURITY CLASSIFICATION OF THIS PAGE(When Data Entered)

volatile-product formation. The temperature at which the high-temperature process occurs coincides with that for decomposition of the perfluoro-substituted benzoxazoles. Some of the other samples analyzed include acetylene-terminated imides and quinoxolines. No appearance of volatile products from the imides or quinoxolines was noted at or below the curing temperature (~ 200°C).

UNCLASSIFIED

SECURITY CLASSIFICATION OF THIS PAGE(When Data Entered)

PREFACE

This report was prepared by Dr. E. G. Jones and Mr. Paul Benadum of the Research Applications Division of Systems Research Laboratories, Inc., 2800 Indian Ripple Road, Dayton, Ohio 45440, under Contract No. F33615-72-C-1537. The contract was initiated under Project No. 7340, "Nonmetallic and Composite Materials," Task No. 734004, "New Organic and Inorganic Polymers." It was administered under the direction of the Air Force Materials Laboratory, Wright Patterson Air Force Base, Ohio, with Dr. Ivan J. Goldfarb, AFML/MBP, as Project Scientist.

The studies outlined in this report were conducted in the Air Force Materials Laboratory during the period April 1974 through March 1975. The experiments were performed by Mr. P. A. Benadum, and the analyses were conducted by Dr. E. G. Jones. This study is a continuation of studies initiated earlier under this contract. The preliminary results were reported in a previous technical report AFML-TR-74-178. This report was submitted in June 1975.

The authors would like to acknowledge the efforts of Mr. Tom Apple, Dr. D. T. Terwilliger, and Mrs. M. Whitaker of the Research Applications Division of Systems Research Laboratories, Inc., and the computer assistance of Mr. G. Doll, University of Dayton Research Institute, throughout the course of this study. The close cooperation and valuable scientific discussions with Dr. Goldfarb and his fellow scientists at the Polymer Branch, Air Force Materials Laboratory, are gratefully acknowledged.

TABLE OF CONTENTS

SECTION		PAGE
I	INTRODUCTION	1
II	INSTRUMENT STATUS	4
	A. Vacuum System	4
	B. System Electronics	19
	C. Data-Acquisition System	25
	D. Isothermal Aging Apparatus	25
III	EXPERIMENTAL RESULTS	27
	A. Introduction	27
	B. Example of Data Output	27
	C. Reports on Sample Analyses	29
	D. Fluorocarbon Elastomer Series	72
IV	FUTURE PLANS	79
	REFERENCES	80

LIST OF ILLUSTRATIONS

FIGURE		PAGE
1	Pumping System (CVC, 2-in.)	5
2	Machining Diagrams for (a) Balance Electrical Feedthrough, (b) Ionization-Gauge Connection	7
3	Schematic of Multiple-Cross Geometry	8
4	Multiple-Cross Dimensions in x-z Plane	9
5	Multiple-Cross Dimensions in x-y Plane	10
6	Machining Diagram for 6-in. Flange	11
7	Pumping System (NRC, 2-in.) and Cross Geometry	12
8	Baseplate Flange Location	14
9	Foreline Pumping Configuration	16
10	Double-Sided Conflat Dimensions	17
11	Thermocouple Configuration	18
12	Schematic Diagram of Data System	20
13	Digital Sweep Circuit	21
14	Data Latches	23
15	Memory Select Circuit	24
16	Percent Weight Loss (Experiment No. 67)	30
17	First Derivative of Weight Loss (Experiment No. 67)	31
18	Total-Ionization Current (Experiment No. 67).	32
19	First Derivative of Weight Loss and Total-Ionization Current (Experiment No. 67)	33
20	Temperature Behavior (Experiment No. 67) of Ions m/e 19, 20	34
21	Temperature Behavior (Experiment No. 67) of Ions m/e 27, 28	35
22	Temperature Behavior (Experiment No. 67) of Ions m/e 29, 31	36

LIST OF ILLUSTRATIONS (continued)

FIGURE		PAGE
23	Temperature Behavior (Experiment No. 67) of Ions m/e 44, 47	37
24	Temperature Behavior (Experiment No. 67) of Ions m/e 50, 51	38
25	Temperature Behavior (Experiment No. 67) of Ions m/e 66, 69	39

LIST OF TABLES

TABLE		PAGE
1	Supplement to Cable-Wiring List	26
2	Summary of Polymer Samples Analyzed	28
3	Fluorocarbon Formulae	73
4	Temperatures of Sample Evolution: Fluorocarbons	74
5	Temperature of Sample Evolution: Fluoroethers	75
6	Onset Temperature for Ether Fragmentation	78

SECTION I

INTRODUCTION

Material stability in an operational environment is of paramount importance in determining the lifetime of the individual components which are integral parts of an aircraft or missile system. In the design and lifetime prediction of these systems, important information such as material response to excessive heat or exposure to corrosive or other reactive environments is essential. The present study focuses on temperature and its effects in the decomposition of polymeric systems.

A knowledge of decomposition products is the first step in the determination of a degradation mechanism. By analyzing the products and the conditions under which degradation occurs, important insight into the chemical changes can be gained. Some understanding of the chemistry of the degradation process makes possible the prediction of new designs for more stable systems. In this manner general stability criteria are evolved which may serve in the design and production of polymers for use over an extended operational temperature range. Extension of the temperature stability range is economical and provides a wider margin for fail-safe operation in a critical environment.

Analysis of materials in their normal operational environment is extremely difficult since the extent of structural deterioration over a period of weeks or even months may be negligible. Systems which decompose infinitesimally are usually the most difficult to analyze; therefore, in the laboratory the temperature conditions must be grossly different from those in the normal operating state. Such experiments are commonly conducted in two ways. In the first, the sample temperature is gradually elevated from ambient to a level at which most of the sample has decomposed; in the present study the time required for this temperature change is ~ 4 hr. Here the assumption is made that in the laboratory case of a rapid temperature change, the chemical and physical changes observed can be correlated with decomposition at lower temperatures over a considerably longer time span. In the second type of experiment, the sample is studied at a fixed elevated temperature under conditions approaching isothermal for periods in excess of one week. In

many instances these experiments can be correlated to provide an overall view of polymer stability.

Frequently sample weight is monitored as a function of temperature [thermogravimetric analysis (TGA)]. This provides information concerning the temperature region over which decomposition occurs. Such experiments are useful in a gross characterization or in the case of stability determination. Recently, more sophisticated studies have been performed in which TGA is combined with gas chromatography (GC) and/or mass spectrometry (MS). The combination TG-MS has been employed in a cooperative effort by the Polymer Branch of the Air Force Materials Laboratory (AFML/MBP) and Systems Research Laboratories, Inc. The mass spectrometer is a powerful tool for monitoring degradation products. Of the mass spectrometers available, the quadrupole mass spectrometer is quite compact, has high ion transmission, and is capable of very rapid mass-spectral scans over a wide mass range.

Multiple product formation at one particular temperature complicates the identification because of overlap of the mass-spectral peaks. Four methods may be employed to simplify the situation, each having distinct advantages and disadvantages. A high-resolution mass spectrometer¹ may be used to separate the individual isotopes; however, these instruments are costly and good relative intensity comparison at high resolution over a wide mass range requires slow mass scans. With a second method, GC-MS coupling,² complete separation of all of the components injected at one time is possible; unfortunately, GC separation requires long periods of time. Thus, although GC-MS can provide very precise identification of products evolved at one particular temperature, the intervals between GC sample injections result in a considerable loss of valuable data. A third method involves using secondary ionization such as chemical ionization (CI) to produce CI spectra which may help in distinguishing the individual mixture components. A fourth technique involves computer analysis³ of the mass spectra to compare the unknown mixtures with a tabulated mass-spectral library of standards.⁴ With the present system, the final technique is the most practical approach.

This report covers results obtained during the period April 1974 to March 1975. Considerable improvements in both the instrument operation and data analysis have been effected over this period. The former improvements include those already complete, some still in the process of being completed, and those that are being proposed for the near future. The latter includes improved data output and the introduction of mass-spectral interpretation of the data. In addition to the TG-MS studies, this report deals with the isothermal aging apparatus which was also constructed for the Air Force Materials Laboratory by Systems Research Laboratories, Inc.

SECTION II
INSTRUMENT STATUS

The present operation schedule permits two complete sample analyses per week. One day is required for complete sample preparation and pumpdown, one day for the experiment, and one day for computer turnaround. This rate of analysis is sufficient to accommodate samples at the present inflow; however, changes in the system operating characteristics can greatly shorten the sample-analysis period. The following series of mechanical and electronic modifications are in progress to improve the instrument efficiency and thus accommodate more samples. Some of these modifications have recently been completed and others are in the design stage. The major thrusts are in the areas of the vacuum system and the quadrupole mass-scan procedure.

A. VACUUM SYSTEM

Changes in progress to improve the vacuum pumping system were designed to significantly shorten the initial pumpdown time, improve quadrupole operating characteristics such as resolution and sensitivity, and provide experimental versatility.

1. Two changes have been made in the venting procedure. First, the vent has been moved to the high-vacuum side of the diffusion pump to permit uninterrupted operation of both rotary and diffusion pumps. Second, dry nitrogen rather than air is now being used as a venting gas.

2. Presently the 2-in. CVC diffusion pumping lines are constricted to 1.3 in. over a distance of ~ 2 ft. As a result of the limited conduction, evacuation of the large bell jar (vol. = 20 ℓ) is time consuming. The solution involves repositioning the 2-in. pump closer to the principal pumping volume and enlarging the connecting lines to improve the pumping speed of the system. Relocation of the 2-in. CVC pump as shown in Fig. 1 is planned. The pumping station is unaltered up to the gate valve, and the system is attached via a T equipped with Varian Conflat flanges to pump the bell jar. Formerly this bell-jar port was used for the balance electrical feedthrough. The third leg of the T will handle an improved electrical feedthrough (Sparrell

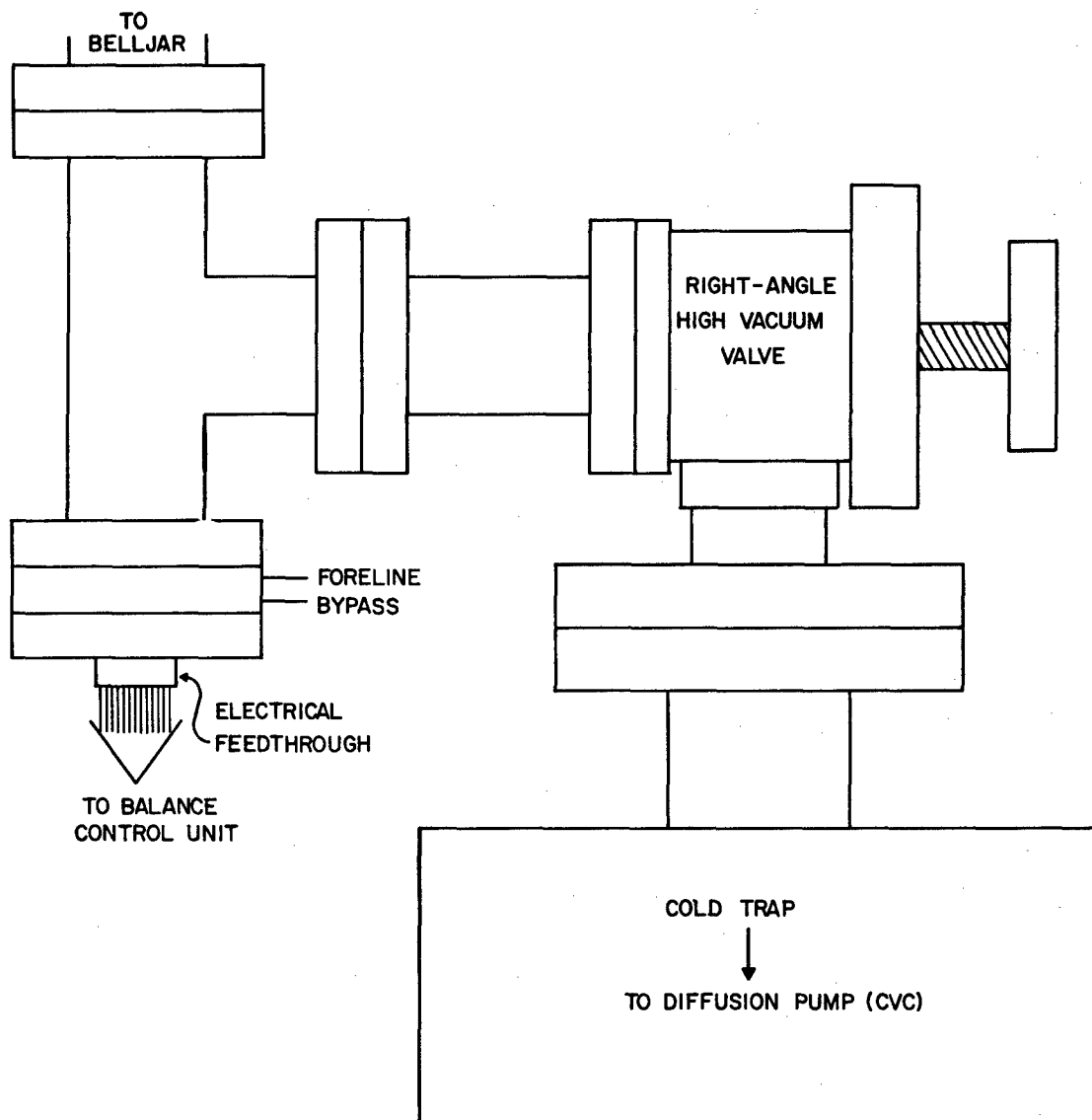


Figure 1. Pumping System (CVC, 2-in.)

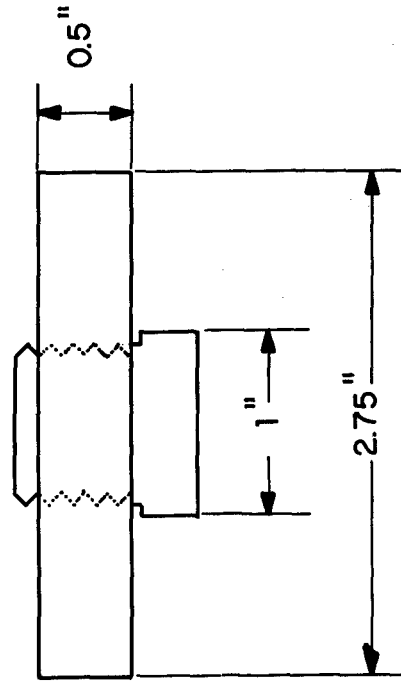
Engineering) having Teflon-coated leads epoxied into a pipe fitting. Figure 2 is a schematic showing the blank flange and feedthrough. Relocation of the pump effects approximately a factor of three increase in gas conductance and a corresponding factor of two increase in effective pumping speed.

3. Two regions require extra pumping. The first is the bell jar which has a large volume and large balance surface area. This must be vented for each sample introduction; as a result, its rate of evacuation determines the system pumpdown time. The objective of the modification outlined above is to permit rapid evacuation of the bell jar. The second region of importance is the multiple cross which unites the sample, quadrupole, balance, and pumping line. Currently, the system pressure during experiments exceeds 5×10^{-5} torr due to sample degradation. At these pressures scattering within the quadrupole and space-charge effects within the ion source can seriously degrade the ion-detection efficiency. In addition it is desirable to operate the electron multiplier at low pressures in order to reduce the occurrence of secondary effects within the multiplier. For these reasons a higher pumping speed in the multiple-cross region is imperative.

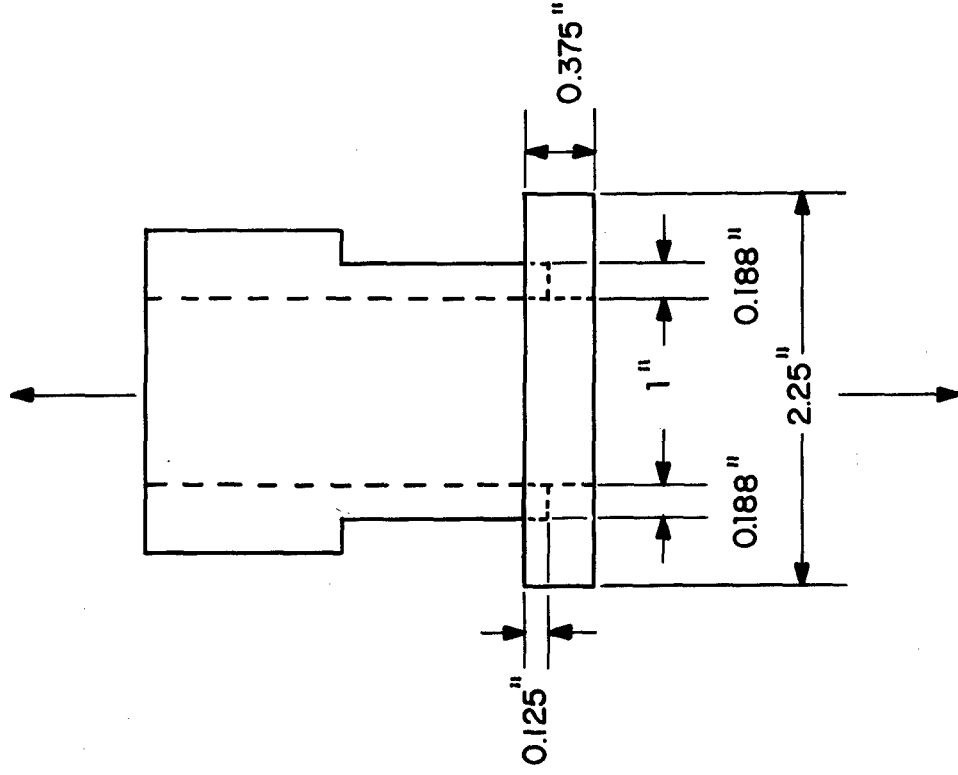
4. A new multiple-cross system has been designed and is currently being assembled. Figure 3 is a schematic of the cross geometry. Figures 4 and 5 are side views of the dimensions in the x-z and x-y planes. Basically the cross is designed to accommodate the quadrupole, balance, and hangdown tube, all having 2.5-in. Conflat flanges. The other three ports are ~ 2.3-in. i.d. and have 4.5-in.-o.d. Conflat flanges. These enlarged ports will accommodate a higher-pumping-speed system.

5. A 2-in. NRC pumping station which has been assembled consisting of a 2-in. NRC diffusion pump (i.d. ~ 3.3 in.), a 2-in. NRC water baffle, and a manually operated Airco gate valve. The pumping speed of this system is ~ 80 l/s^{-1} . The gate-valve flange has been modified to accept a quick-disconnect fitting to an ionization gauge (Fig. 2B). A commercial T with 4.5-in.-o.d. flanges has been heliarc welded to a modified 6-in. stainless-steel flange as shown in Fig. 6. The overall pumping-system geometry in relation to the multiple cross is shown in Fig. 7.

ELECTRICAL FEEDTHROUGH FLANGE
(TO BALANCE)



QUICK-CONNECT TO ION GAUGE



TO GATE VALVE

(a)

(b)

Figure 2. Machining Diagrams (a) Balance Electrical Feedthrough, (b) Ionization-Gauge Connection

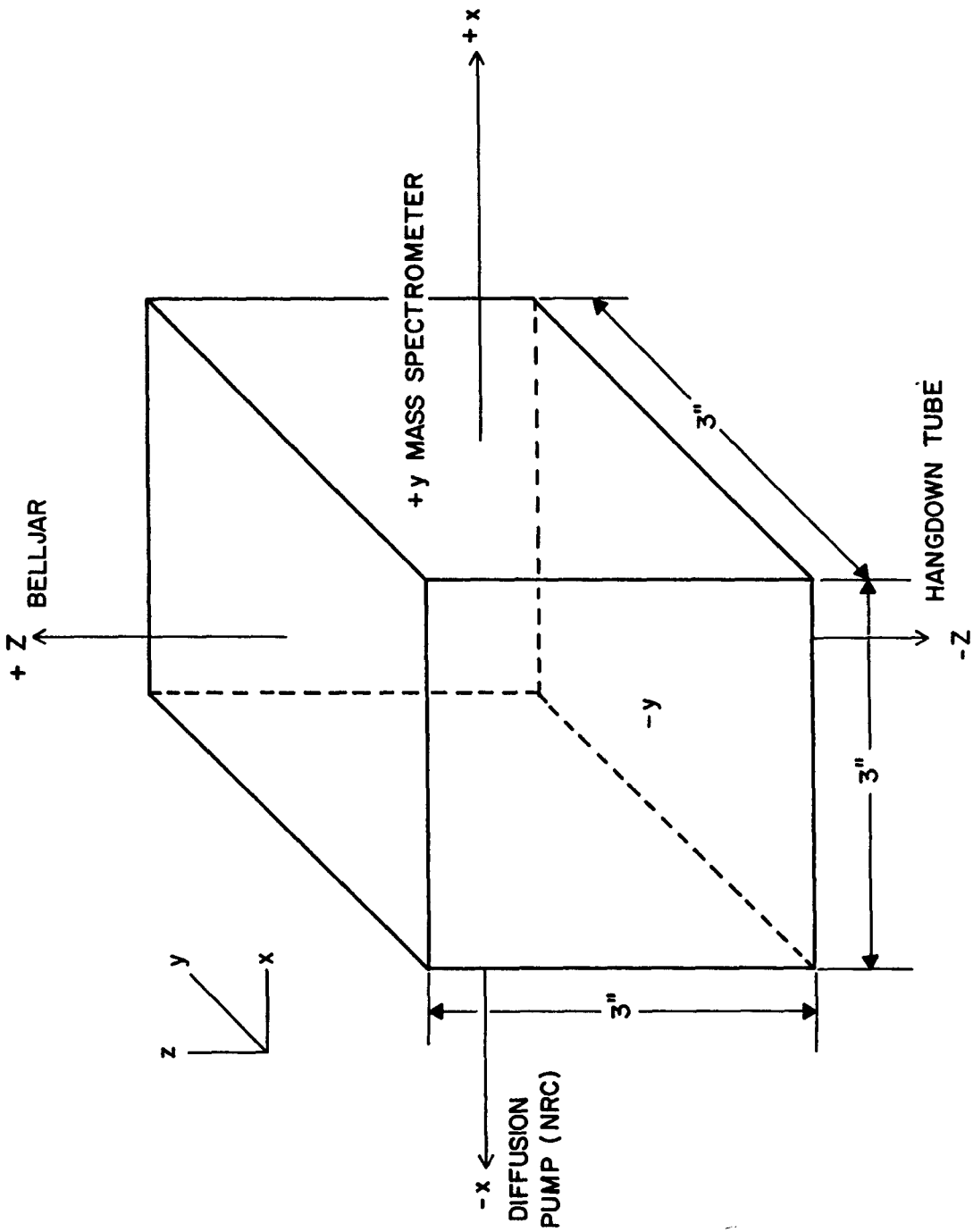


Figure 3. Schematic of Multiple-Cross Geometry

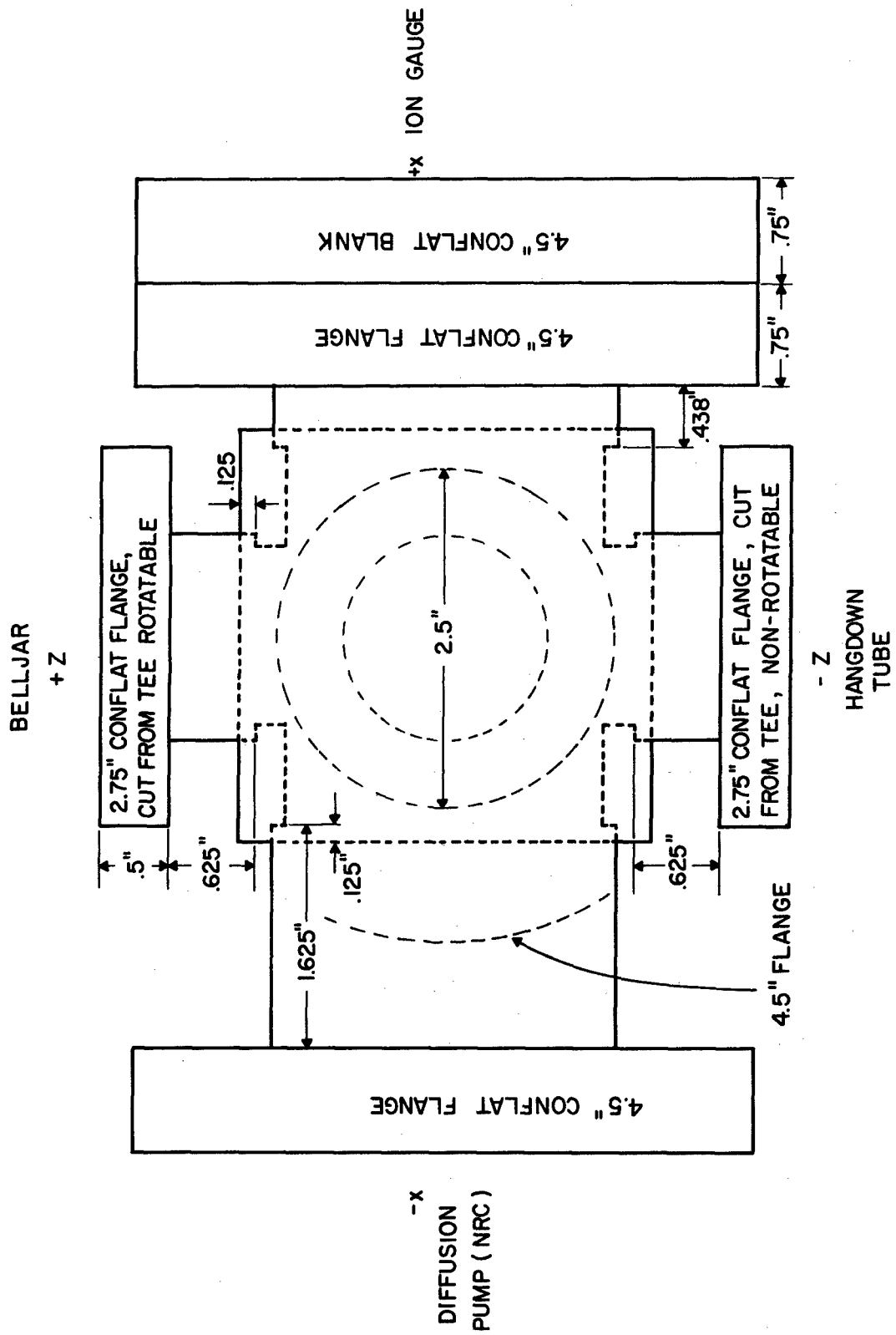


Figure 4. Multiple-Cross Dimensions in x-z Plane

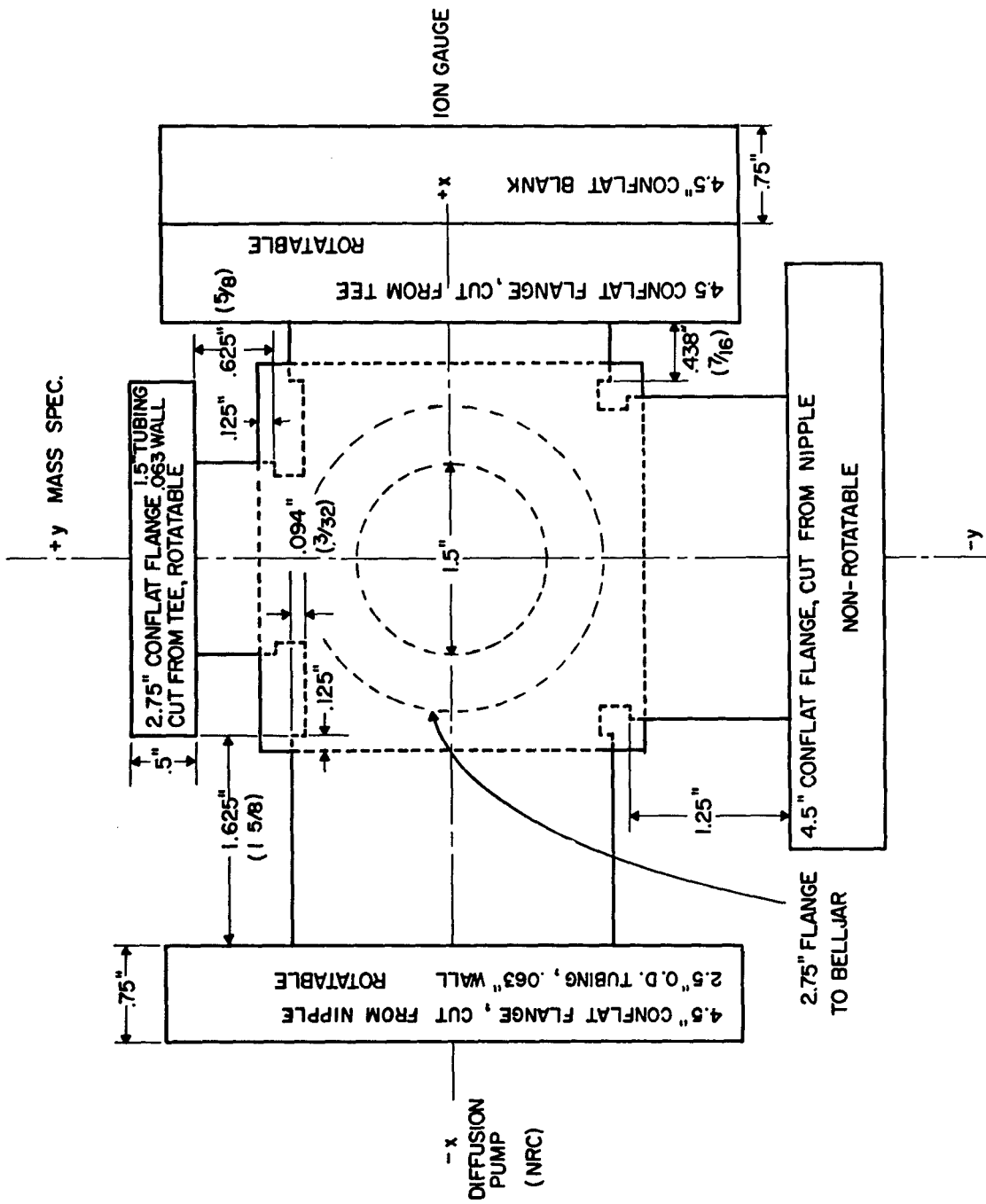


Figure 5. Multiple-Cross Dimensions in x-y Plane

2.5" TEE WELDED TO THIS SIDE OF BLANK

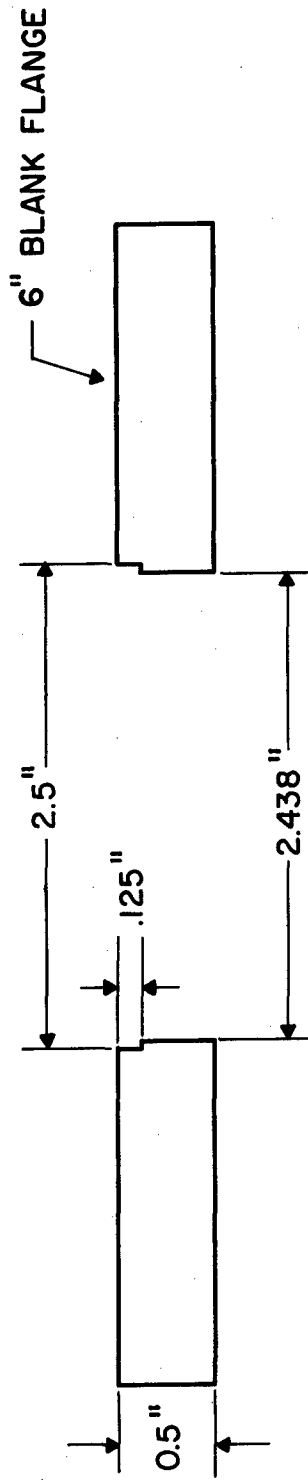


Figure 6. Machining Diagram for 6-in. Flange

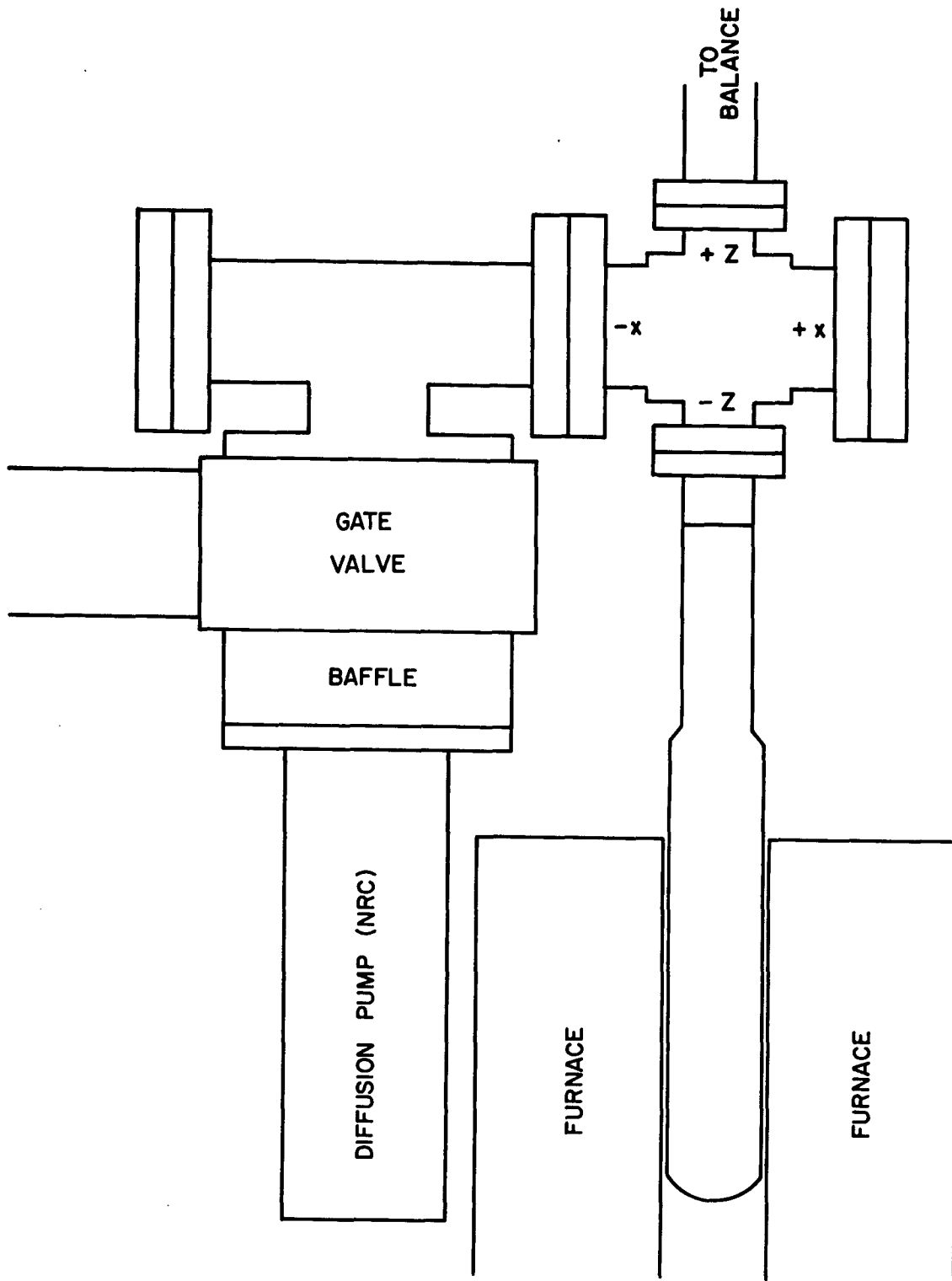


Figure 7. Pumping System (NRC, 2-in.) and Cross Geometry

6. This new design has several important features. First, it provides an effective pumping speed of $\sim 40 \text{ l/s}^{-1}$ at the cross. This improves the pumping speed by one order of magnitude over the original system. For these two isolated pumping systems, the following overall improvements can be listed:

- (i) A 20-fold increase in pumping speed will allow a greatly reduced pumpdown time and thereby increase the sample analysis efficiency.
- (ii) It is conceivable that during an experiment only one diffusion pump may be required. With this system, provision has been made for gating off either pump.
- (iii) The enlarged manifold and direct line of sight along the T through the multiple cross will permit greater experimental versatility. Initially a viewing port (4.5-in.-o.d. flange) can be installed to permit a visual monitoring of the quadrupole and balance wire during an experiment. The line-of-sight feature will permit future experiments in which a sample located at the center of the multiple cross can be impacted with a laser source to permit a TG-MS study of laser interactions with polymers.
- (iv) A third large port will be blanked off initially but will be available for future modifications. In addition this port faces into the quadrupole. This may facilitate maintenance and modifications to the ion source without removal of the entire quadrupole.
- (v) The enlarged manifold will permit a more direct line of sight between the sample and quadrupole ion source. The use of heating tape to continuously heat the multiple-cross region to 70°C is planned.

7. To avoid interference with the multiple cross and to provide an unhindered line of sight, the bell-jar baseplate will be rotated clockwise by 45° from its present position as shown in Fig. 8.

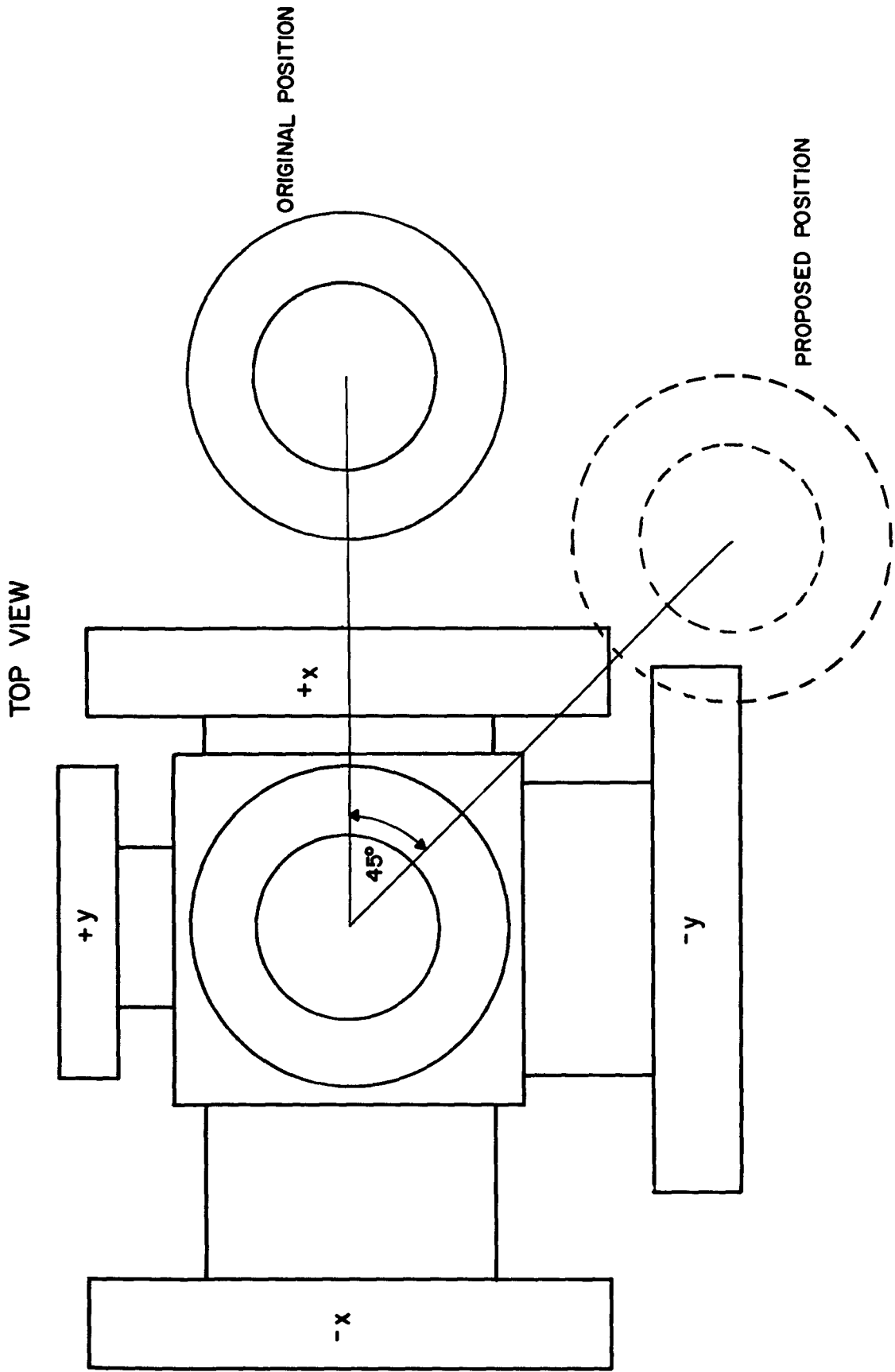


Figure 8. Baseplate Flange Location

8. The foreline pumping arrangement has been redesigned to permit independent operation of the 2-in. pumping systems. Figure 9 is a schematic of the planned system which basically consists of a solenoid valve for power-failure protection, an oil trap and a mini-Conflat cross leading to the two diffusion pumps, and a diffusion-pump bypass roughing line.

9. Currently the Granville Phillips cold trap will operate unattended for ~ 12 hr with a full charge of liquid nitrogen. This interval does not permit safe overnight or weekend operation. A cryocooler (Neslab) has been ordered to replace the liquid-nitrogen function. Its operating temperature (-60°C) is sufficiently low for our requirements, and it will allow continuous operation of the pump.

10. The method of gaseous sample introduction has been improved. A double-sided Conflat has been machined with two entrance ports as in Fig. 10. One leads to a Granville Phillips variable leak valve for standard gas calibration. The second is blanked off initially; however, provision has been made for gas-chromatograph coupling with the mass spectrometer to create a combination TG-MS and GC-MS capability. This Conflat will be located between the hangdown-tube flange and the multiple cross to provide easy access to the quadrupole ionizer. The ports are 0.25-in. stainless-steel; however, a high-temperature ferrule fitting will provide uninterrupted 0.125-in.-tubing access from a chromatograph through the vacuum system to the vicinity of the ion source.

11. To incorporate more precise temperature measurement, a room-temperature compensator for a Pt/Pt-10% Rh thermocouple has been installed. To avoid complications for the thermocouple vacuum feedthrough leads, the compensator was located in the vacuum as shown in Fig. 11. No excessive degassing problems were experienced in the initial tests.

12. A vacuum protection system based on the ionization gauge has been installed; manual override is available.

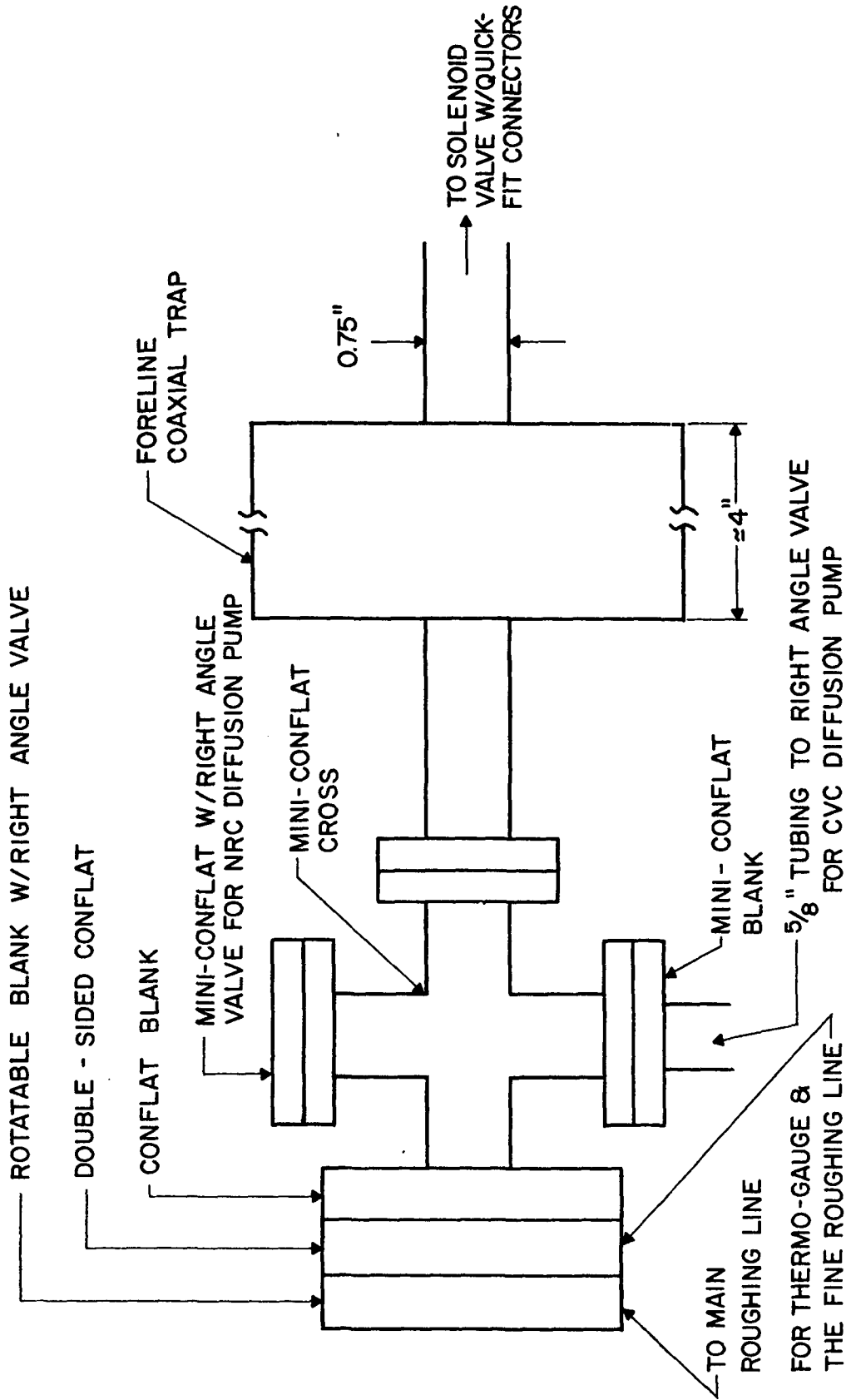


Figure 9. Foreline Pumping Configuration

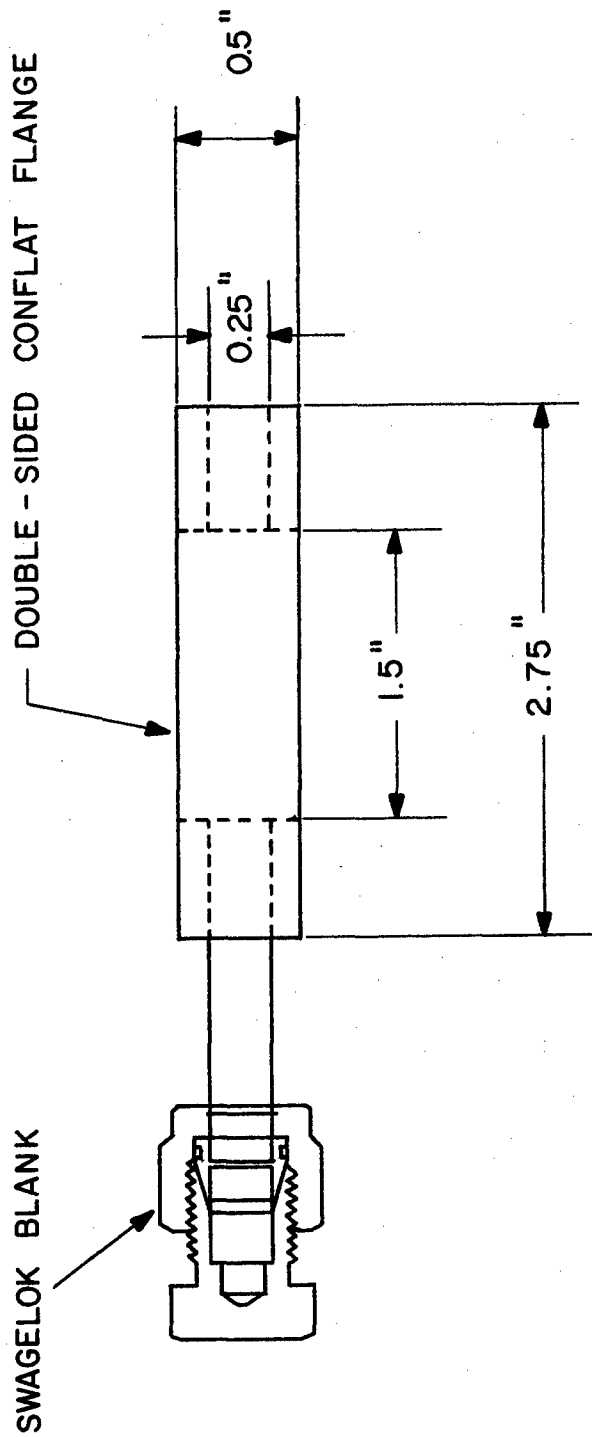


Figure 10. Double-Sided Conflat Dimensions

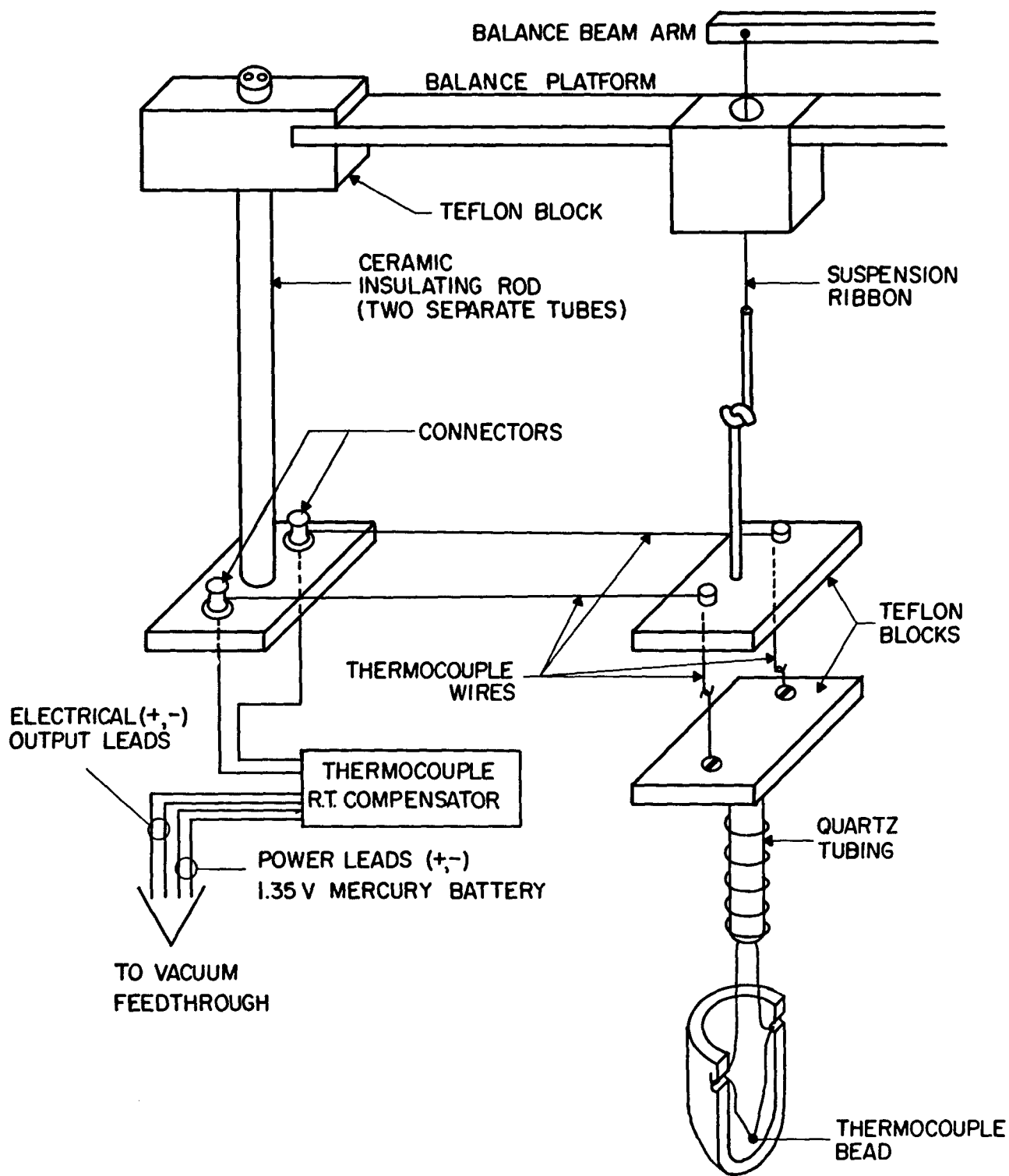


Figure 11. Thermocouple Configuration

B. SYSTEM ELECTRONICS

The method of mass sampling is presently being altered. Some of the components have been assembled; however, in general these will not be ready for installation for several months. A diagram of the electronic data system is shown in Fig. 12.

1. Digital Sweep Circuit. The digital sweep circuit (Fig. 13) will allow the mass-spectrometer ramp voltage to be stepped along the peaks of each individual mass rather than scanned continuously. This eliminates the need for computer determination of the peaks and their identification. This will also eliminate false peaks (originating from noise) and half masses originating from doubly charged ions. The MTA computer program, therefore, would no longer be necessary. Also, the amount of data recorded on magnetic tape would be only 10% of that presently required. This would allow the use of a smaller tape or the recording of a large volume of data. This design is tentative and subject to change.

In order to step the ramp voltage, a digital-to-analog converter (DAC) will be used. To obtain the desired resolution between masses and to insure stepping as close as possible to the center of the mass peak, a 16-bit binary-input DAC has been chosen. Stepping is provided by a binary counter using 74193 presettable four-bit binary counters. A code conversion is necessary to change the binary count to the digital code required by the DAC for production of a ramp voltage for a given mass. In other words, a count of 12 at the input of the DAC will not produce the ramp voltage needed to set the mass spectrometer for mass 12. For generation of the proper binary code for each mass, a reference table will be created with an electrically programmable read-only memory (EPROM). To determine the amount of memory space required, the assumption was made that the number of masses scanned would be ~ 300. With each code requiring 16 bits for generating the voltage for one mass, 4800 bits of storage is required.

This places the memory capacity between 4096 (4K) and 8192 (8K) bits. A standard 4K memory then would be insufficient and an 8K memory would be more than sufficient. To obtain the 8K bits, either two 4K memories can be used as shown in Fig. 13 or one 8K memory (just now on the market). An 8K

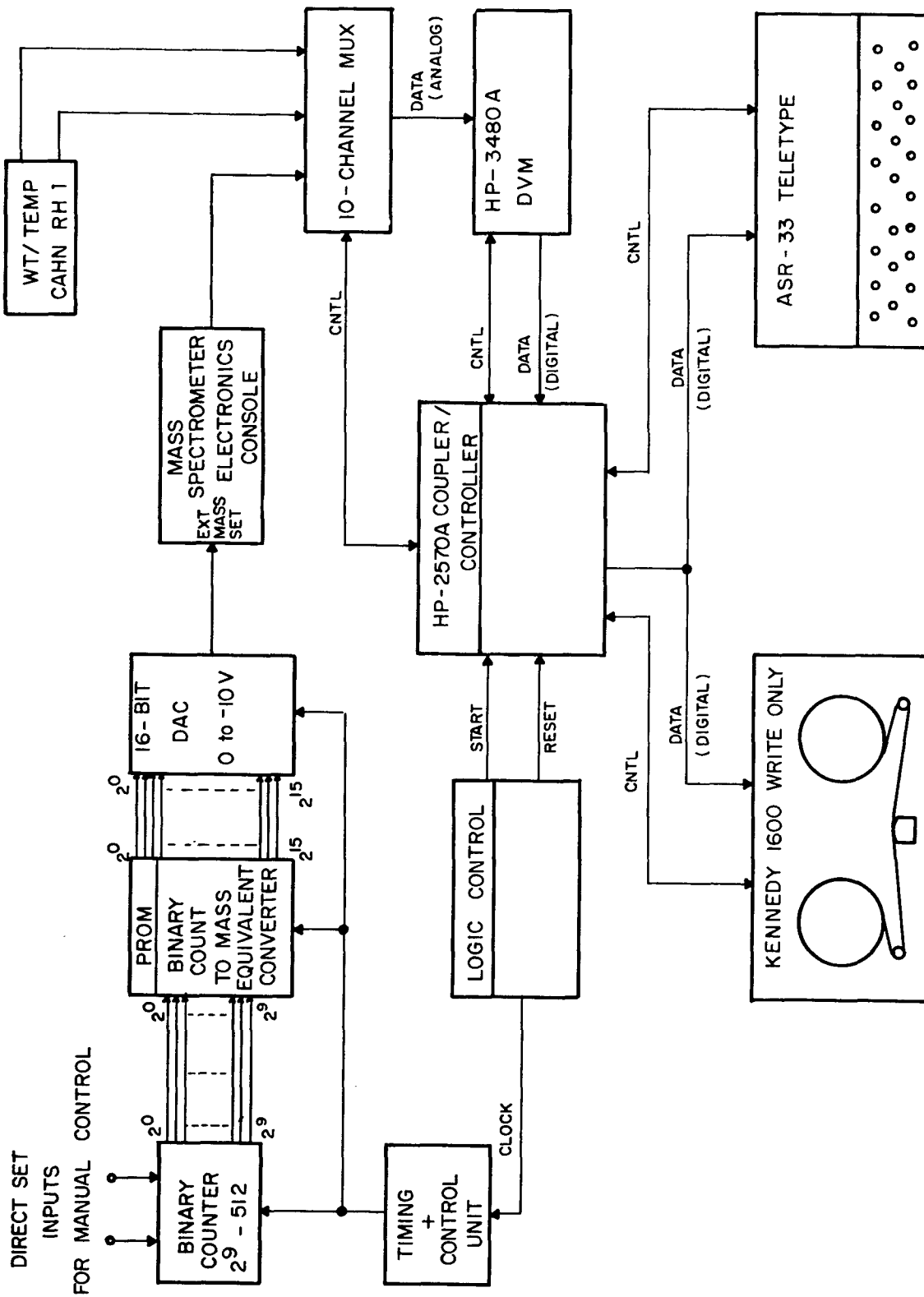


Figure 12. Schematic Diagram of Data System

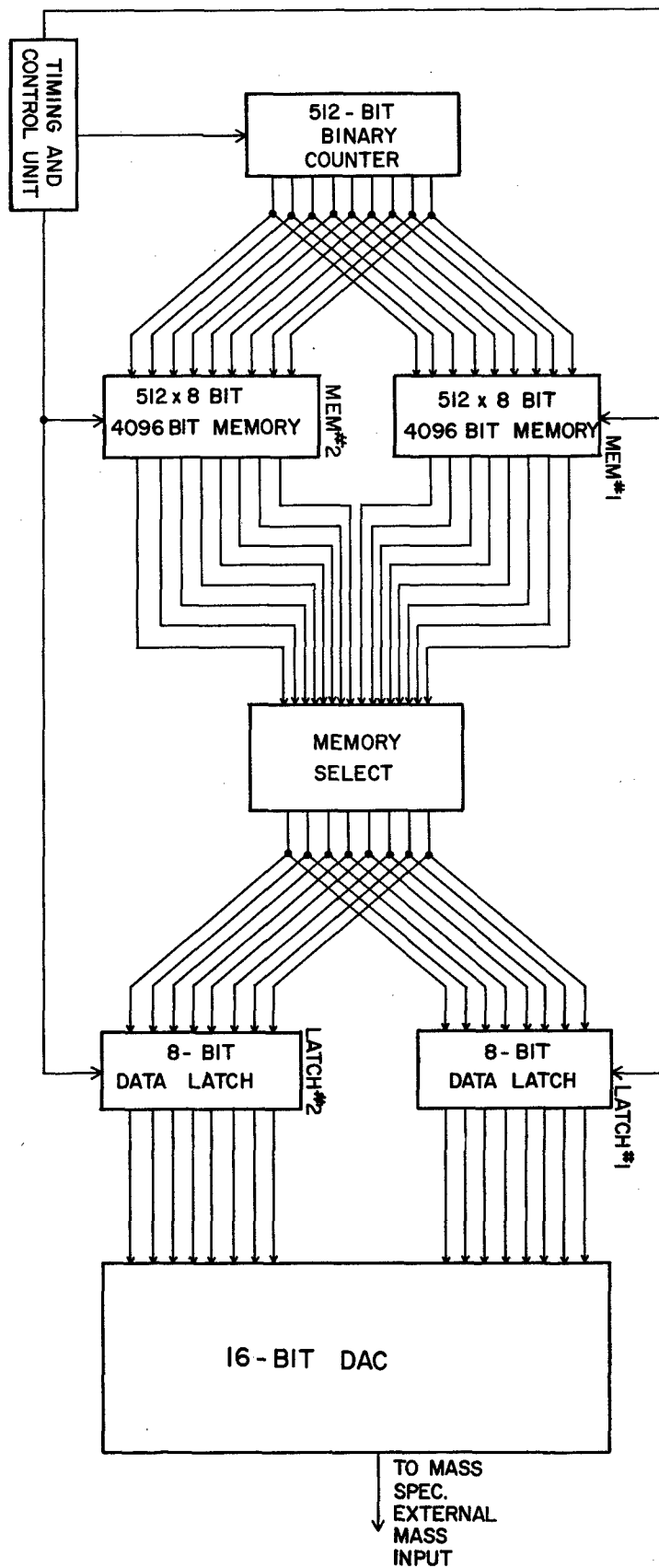


Figure 13. Digital Sweep Circuit

EPROM is now under consideration, but the description of the circuit operation will be confined to the two-4K-memories situation.

Two 4K memories (National Semiconductor MM5204) were selected for the code conversion. Each memory is arranged as 512 words by 8 bits/word. To obtain an entire 16-bit word, two consecutive memory locations are used. This essentially makes it a 256 x 16 memory. Each 8-bit word is held in a data latch (Fig. 14) while the 16-bit word is being formed. Their outputs are presented to the DAC which sets its output according to the code. It can be seen that for each mass conversion, the memory is stepped twice. Each memory has a capacity for 256 mass locations. Since only one memory can be used at a time, a method must be devised for memory selection. The MM5204 utilizes Tri-State Logic which allows common data bussing. Each memory has a chip enable input which is used to place the data on the output lines. By controlling the state of the chip enable lines, the memories can be selected at will. Figure 15 shows an alternate method of memory selection.

Since two memory locations are required for generation of each 16-bit word, some means must be provided for storage of the bits in order that the entire word can be presented to the DAC at one time.

Four quad latches (7475) act as storage registers for the data bits. Each 7475 contains four bistable latches. Eight latches are used to store the first eight data bits, and another eight latches are used to store the last eight data bits. Two of the quad latches are clocked during any odd memory address, and the other two are clocked during any even memory address. The timing and control unit must be designed and the ramp voltage level determined for each individual mass. Under consideration is the use of the HP-2570A coupler/controller system clock and control lines.

2. Two instrumentation amplifiers are to be added to the data-acquisition system. At the present time, the amplifiers in use are shared with another data system. By eliminating the need for these amplifiers, weight and temperature measurements can be made without interference from the other system.

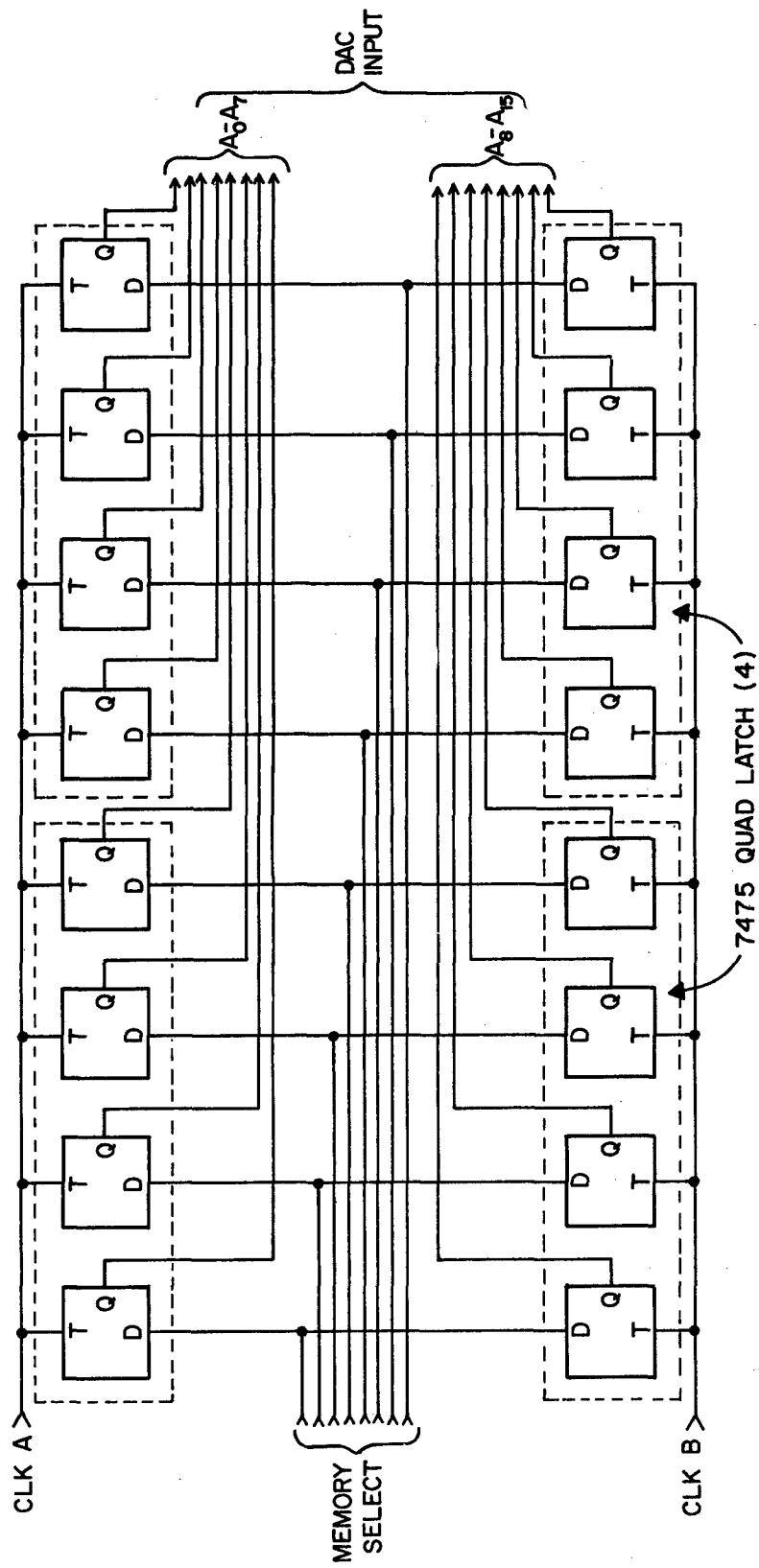


Figure 14. Data Latches

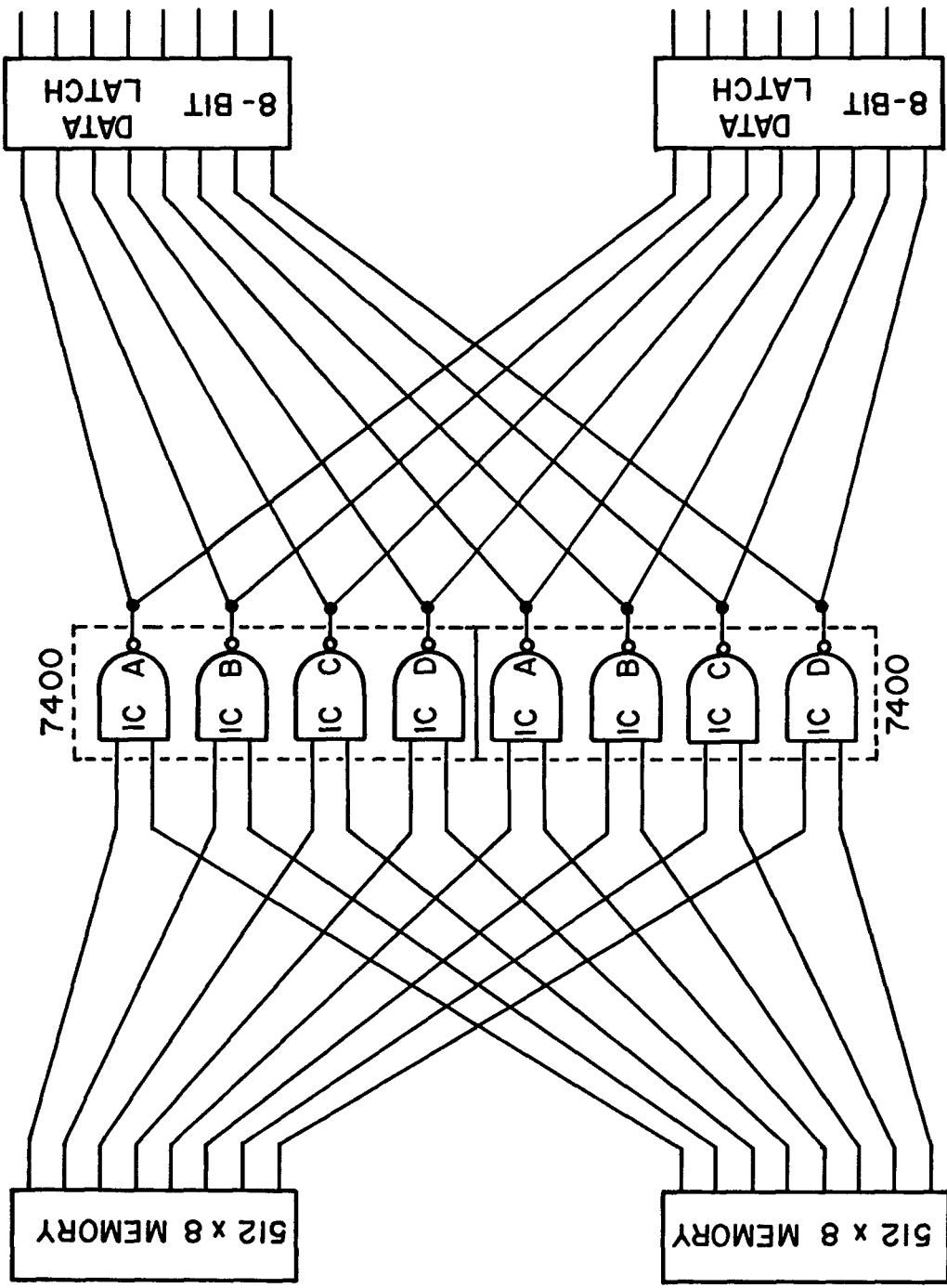


Figure 15. Memory Select Circuit

C. DATA-ACQUISITION SYSTEM

During the course of this study, several suggestions were made for improving the format of the data output. These have resulted in the following changes:

1. Provision has been made for plot of the total ionization current as a function of scan number.
2. Provision has been made for plotting of the first derivative of weight loss.
3. For each scan the computer prints the temperature in degrees Centigrade rather than thermocouple readout in millivolts.
4. The change in intensity format has produced clear scaling factors.
5. Provision has been made for accommodating another factor of ten in ion intensity.

In addition, in order to economize on computer paper usage, the plot routines have been altered in such a way that two ion dependences appear on each plot.

D. ISOTHERMAL AGING APPARATUS

Erratic instrument behavior over an extended period resulted in an overall reassessment of the performance of the aging apparatus. In the course of this investigation, programs were outlined to alleviate electronic, furnace, and electrobalance problems. The extent of this future effort is under consideration at the present time. The Cahn (Model RM2) electrobalance was removed from the apparatus and was rigorously tested for short- and long-term stability under different load conditions approximating the normal operating conditions. These tests indicated a serious balance malfunction which over a period of time had seriously degraded the overall function of the apparatus. This balance was replaced with a second balance (Model DTL 7500) from the same manufacturer.

During the course of instrument troubleshooting, the DPM cabling was rewired. A supplement to the existing cable-wiring list is given in Table 1.

TABLE 1
SUPPLEMENT TO CABLE-WIRING LIST

DTI DPM (30-pin connector)	DTI Data Jack (added) (50-pin, Amphenol)	Data Cable	
		(48-pin, HP)	(50-pin, Cinch)
A	3	2	2
B	5	A	26
C	1	1	1
D	28	4	4
E	26	3	3
F	15	F	31
H	11	6	6
J	9	5	5
K	36	8	10
S	17	BB	34,35
1	7	B	27
3	32	D	29
4	30	C	28
7	13	E	30
9	34	7	9
Base of 2N706	38	H	

In service, 6 January 1975.

SECTION III

EXPERIMENTAL RESULTS

A. INTRODUCTION

Over the period covered by the present report, sixteen different polymer samples were analyzed. Individual reports have been made for each sample concerning the gaseous product analysis and the temperature dependence. Table 2 correlates sample identification, experiment number, and report number.

For cases in which more specific information was required than that resulting from one particular experiment or in cases of experimental failure, the samples were reanalyzed. When a series of related polymers is analyzed, patterns begin to emerge. Although these patterns may not be apparent during analysis of the early members of the series, they emerge after several iterations of pattern recognition followed by further data analysis.

The data presentation in this report consists of three parts. The first (Section III B) contains an example of the format of the data output for one sample; the second (Section III C) is a condensation of the individual reports on the sample analyses. The final section (Section III D) is a comparison of one series of polymers having similar structures -- in particular, the fluorocarbon elastomers.

B. EXAMPLE OF DATA OUTPUT

The form of the current computer output is shown in the following analysis for Sample No. 91-210, i.e., Experiment No. 67.

TABLE 2
POLYMER SAMPLES ANALYZED

Sample			Analysis	
Source	Number	Type	Experiment Number	Report Number
FLH	PPQ4-TS	Resin	50	IA-74
RCE	CD-569-1-31	Elastomer	54	IB-74
RCE	96-151	Elastomer	55	IC-74
RCE	151-80	Elastomer	56	ID-74
RCE	34728-22-1	Elastomer	57	IE-74
RCE	151-85	Elastomer	58	IF-74
FLH	FLH-PI4	Resin	59	IG-74
SLA	SLA-220M	Elastomer	60	IH-74
RCE	151-85	Elastomer	62 (rerun)	II-74
RCE	210-51	Elastomer	63	IIA-75
BK	BK-99-80C	Resin	61	IIB-75
Contractor	HR 600	Resin	64	IIC-75
EWC	EWC-56-391-2A	Elastomer	42	IID-75
WSU	BR-2-111	Elastomer	65	IIE-75
RCE	91-210	Elastomer	67	IIF-75
RCE	95-151	Elastomer	68	IIG-75
RCE	55584-20	Elastomer	69	IIH-75

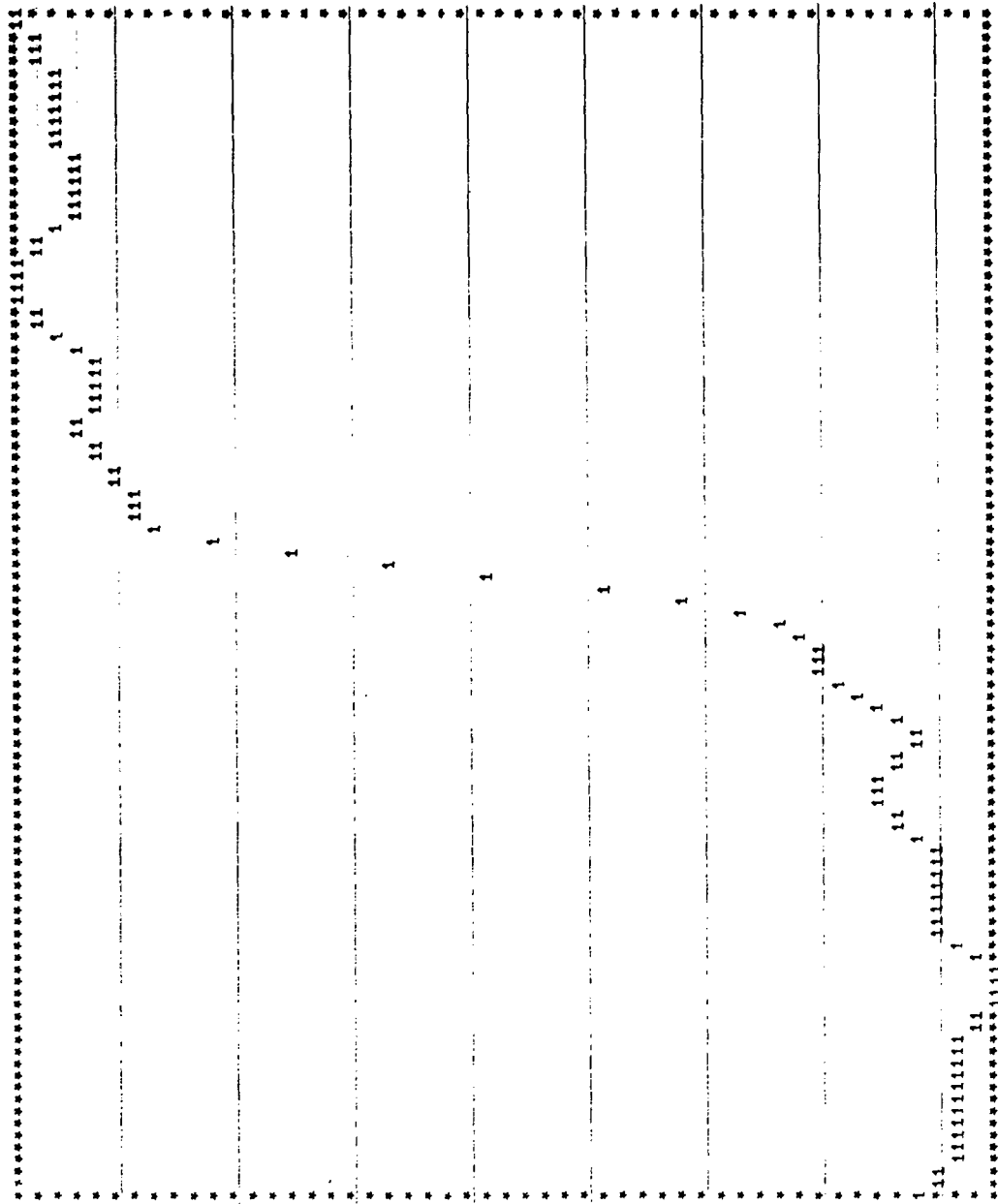
Figures 16, 17, and 18 are plots of the weight loss, the first derivative of the weight loss, and total ionization current, respectively, as functions of scan number. The temperature rises approximately linearly with scan number, beginning at 28 C at the left of the figures and reaching a maximum of 980 C at the extreme right. For details of the analysis, one may refer to the synopsis of Report IIF-75 given in Section IIIC below.

In Figure 19 the first derivative of the weight loss and total ionization are displayed. The former is the distribution of mass evolved, and the latter is a fairly accurate distribution of the volatile species evolved. The former tends to emphasize heavy decomposition products and the latter, the lighter products. Note that these distributions are centered at different temperatures and each has a different half-width (FWHM). The next six figures (20-25) indicate the fragment ionic behavior as a function of temperature. Of interest is the behavior of m/e 69 (Fig. 25) corresponding to CF_3^+ from two different fluorocarbon species. The broad peak at higher temperature arises from carbon tetrafluoride that is formed by a rearrangement reaction. The behavior of m/e 47 (Fig. 23) corresponds to CFO^+ from carbonyl difluoride and other oxyfluorocarbons originating from two different locations in the polymer.

C. REPORTS ON SAMPLE ANALYSES

This section contains abbreviated versions of analysis reports submitted throughout the course of this study. Figures displaying weight loss, total ionization, and specific ion behavior with temperature have been deleted.

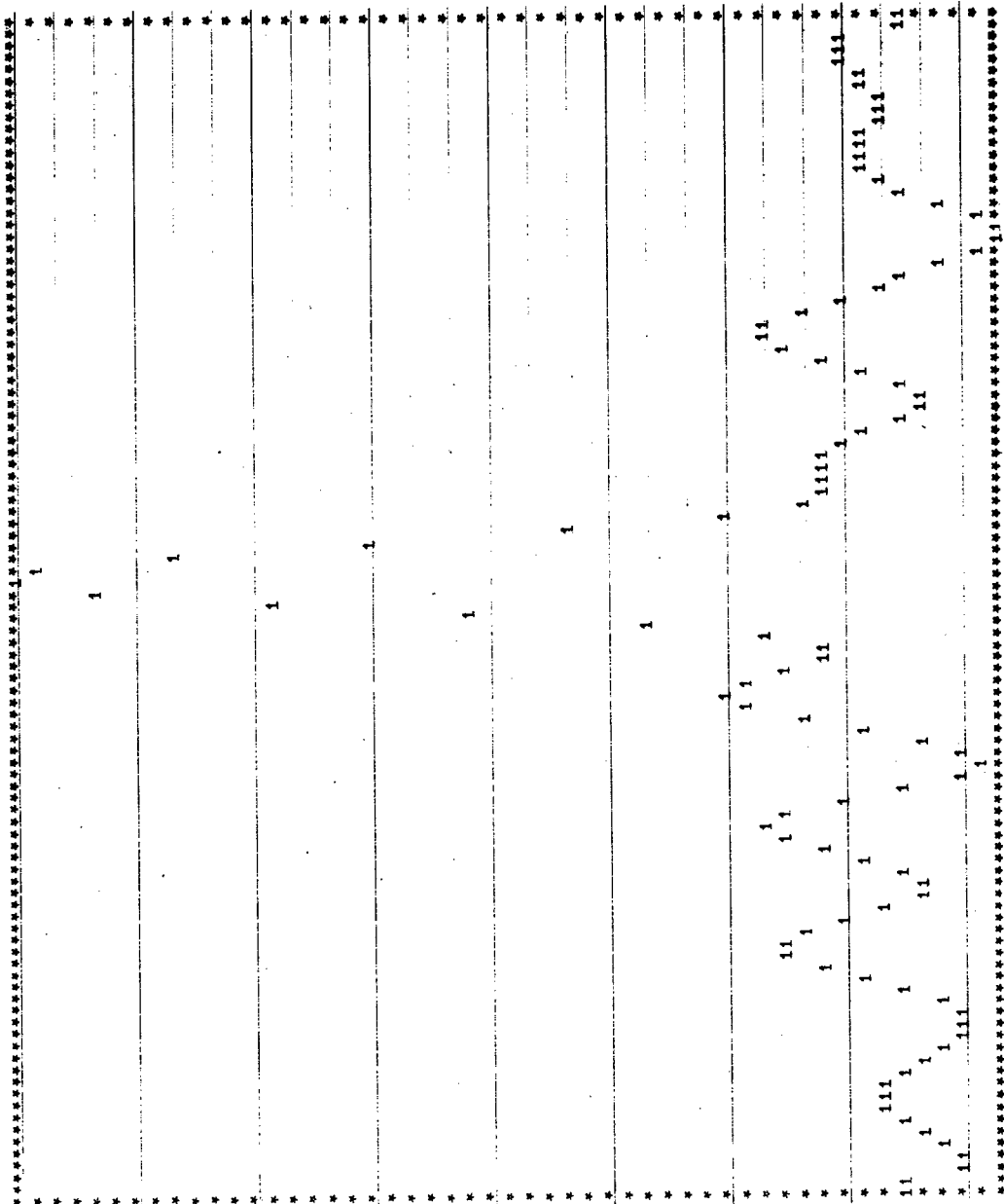
PER CENT WEIGHT LOSS



XFIN = .1000000E+01 XMAX = .1000000E+03 YMTN = 0. YMAX = .1000000E+03

Figure 16. Percent Weight Loss (Experiment No. 67)

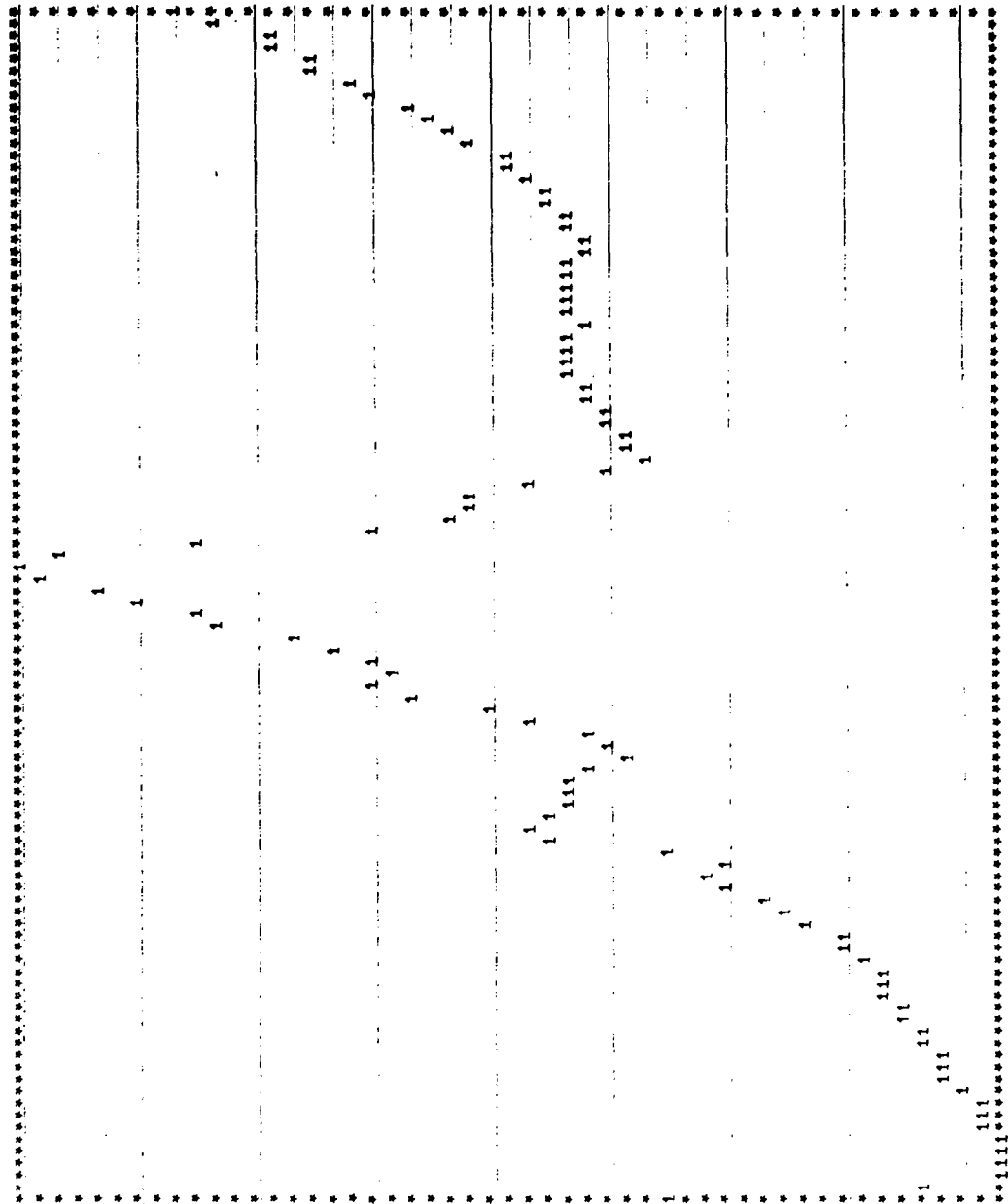
QWOT .US. SCAN NUMBER



XMIN = .1000000E+01 XMAX = .1000000E+03 YMIN = -.52019067E+00 YMAX = .43709699E+01

Figure 17. First Derivative of Weight Loss (Experiment No. 67)

TOTAL INTENSITY VS. SCAN NUMBER



XMIN = .13000000E+01 XMAX = .10000000E+03 YMIN = .10700000E-02 YMAX = .12560000E-01
 XMIN = .13000000E+01 XMAX = .10000000E+03 YMIN = .10700000E-02 YMAX = .12560000E-01

Figure 18. Total-Ionization Current (Experiment No. 67)

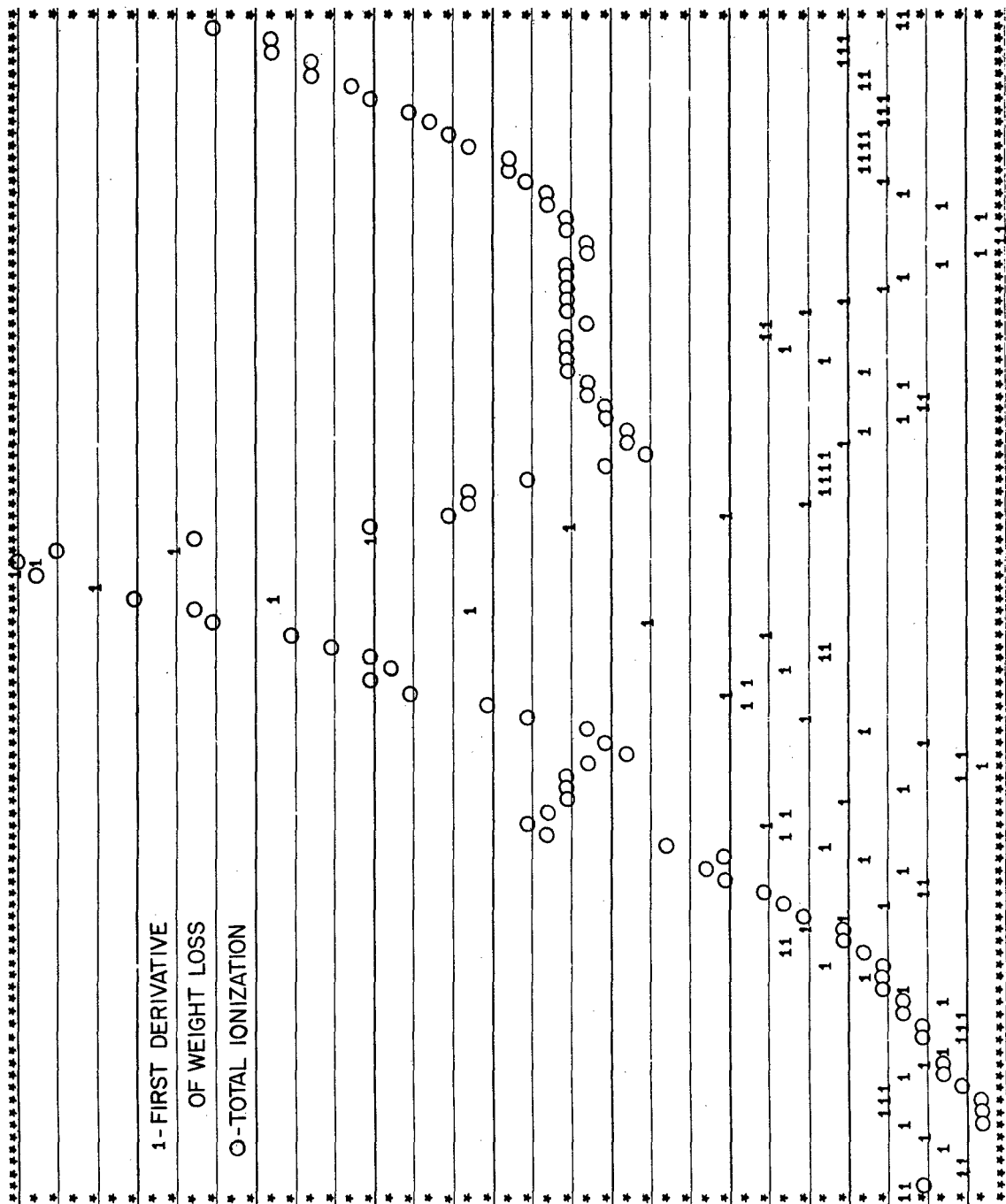


Figure 19. First Derivative of Weight Loss and Total-Ionization Current
(Experiment No. 67)

MASS NO. 19 20
 YMAX = .006 .001

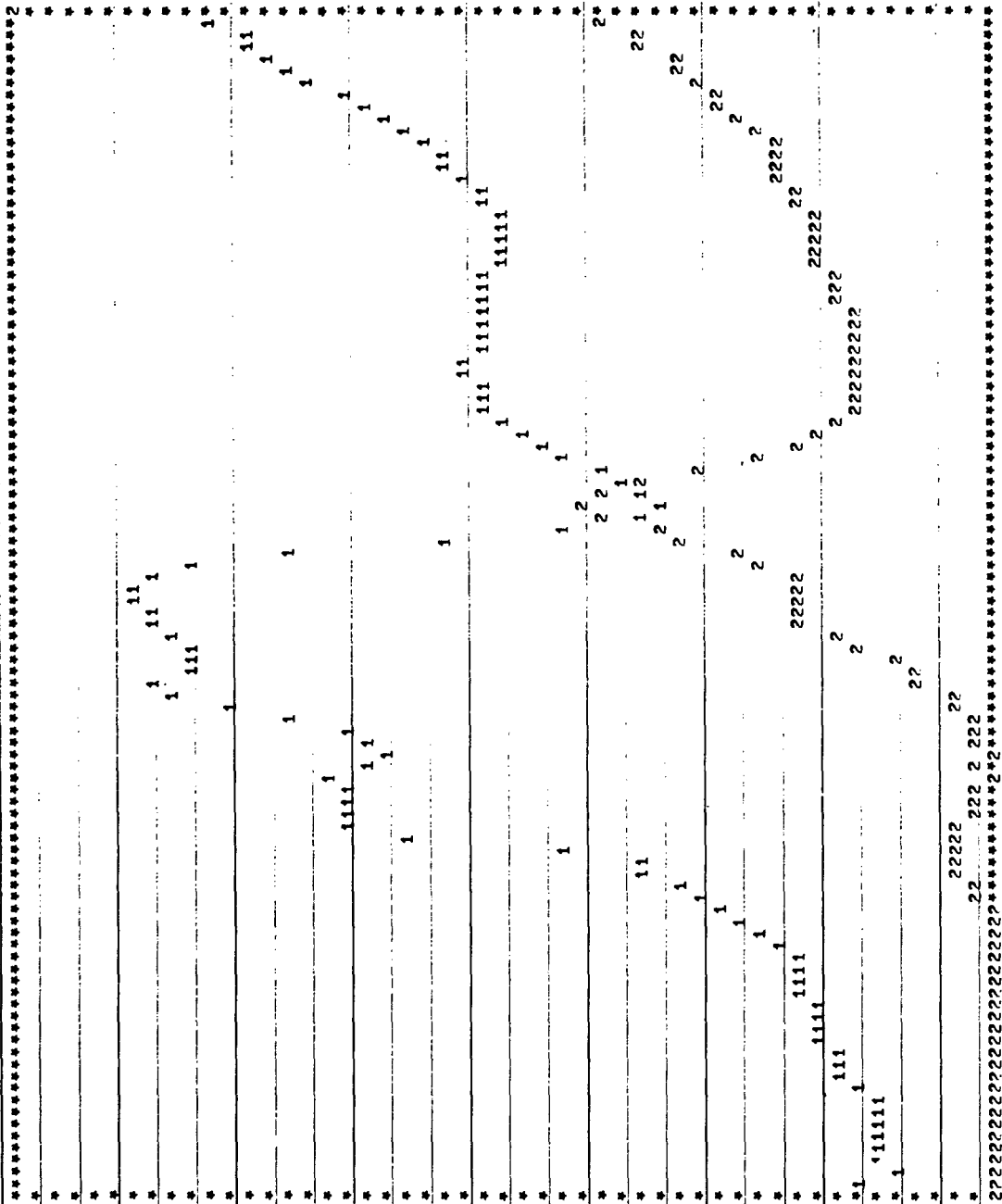


Figure 20. Temperature Behavior (Experiment No. 67) of Ions m/e 19, 20

MASS NO. 27 28
YMAX = .001 .002

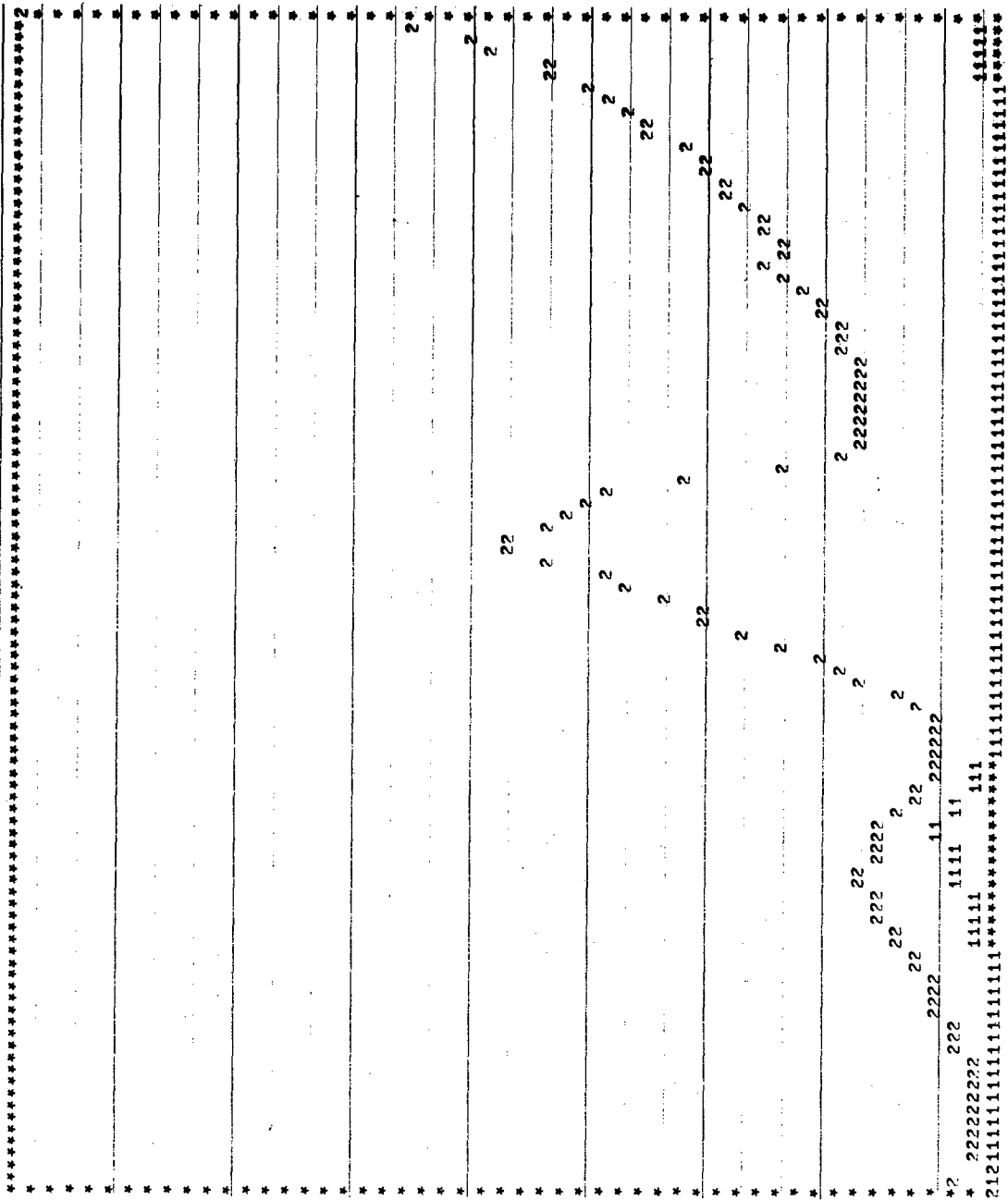


Figure 21. Temperature Behavior (Experiment No. 67) of Ions m/e 27, 28

HASS NO. 29 31
VMAX = .001 .001

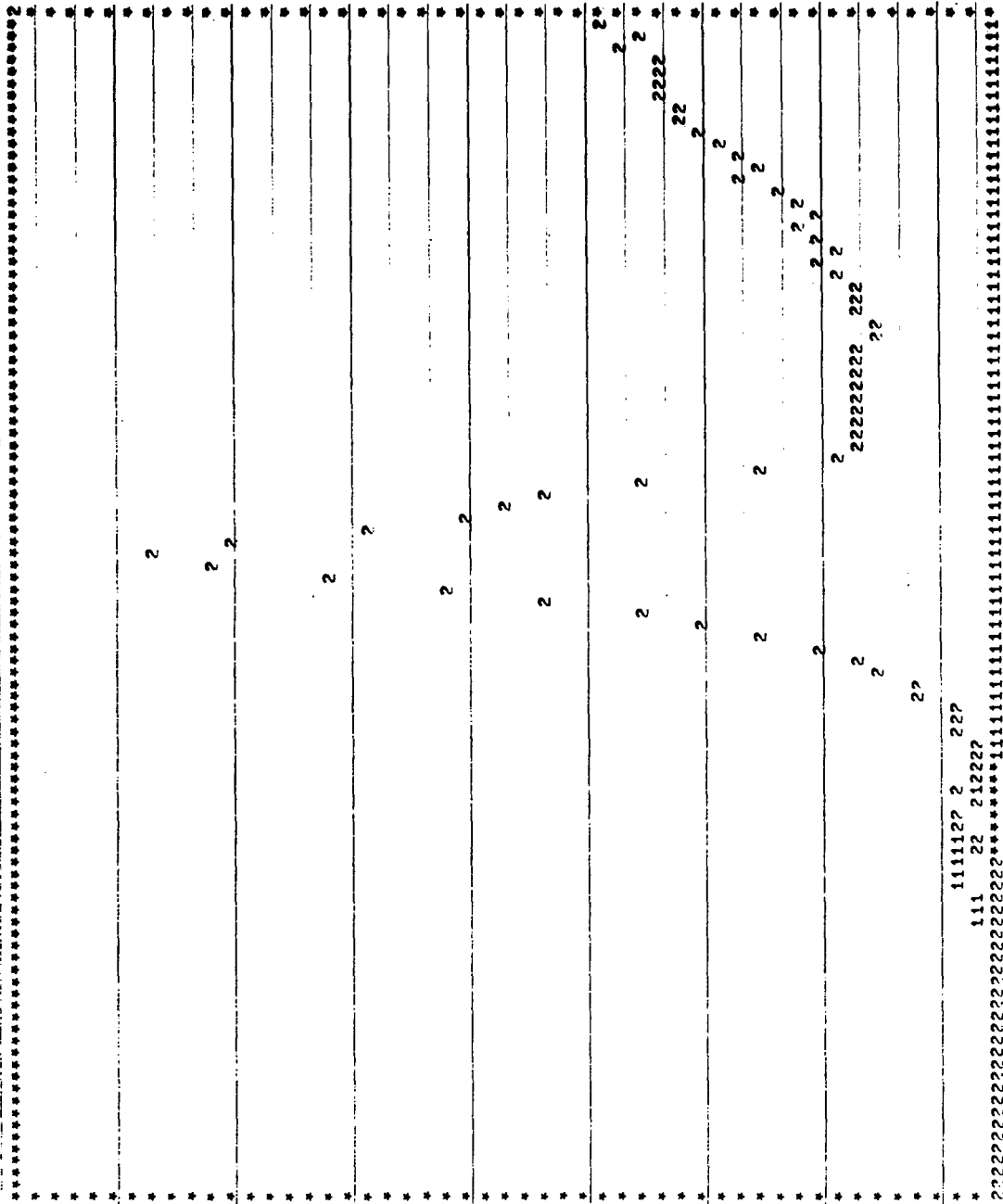


Figure 22. Temperature Behavior (Experiment No. 67) of Ions m/e 29, 31

MASS NO. 44. 47
 YMAX = .001 .001

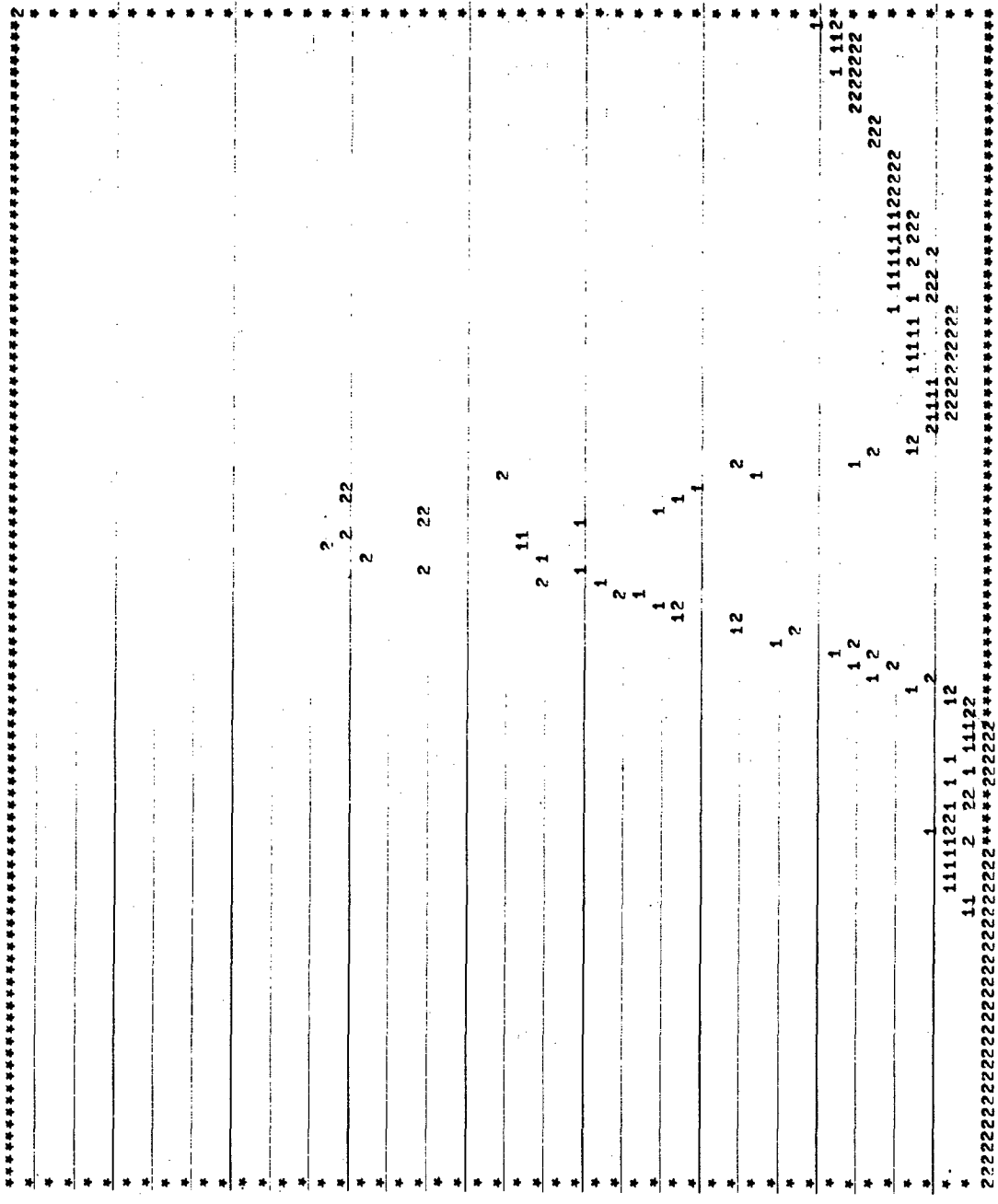


Figure 23. Temperature Behavior (Experiment No. 67) of Ions m/e 44, 47

MASS NO. 50 51
 YMAX = .001 .001

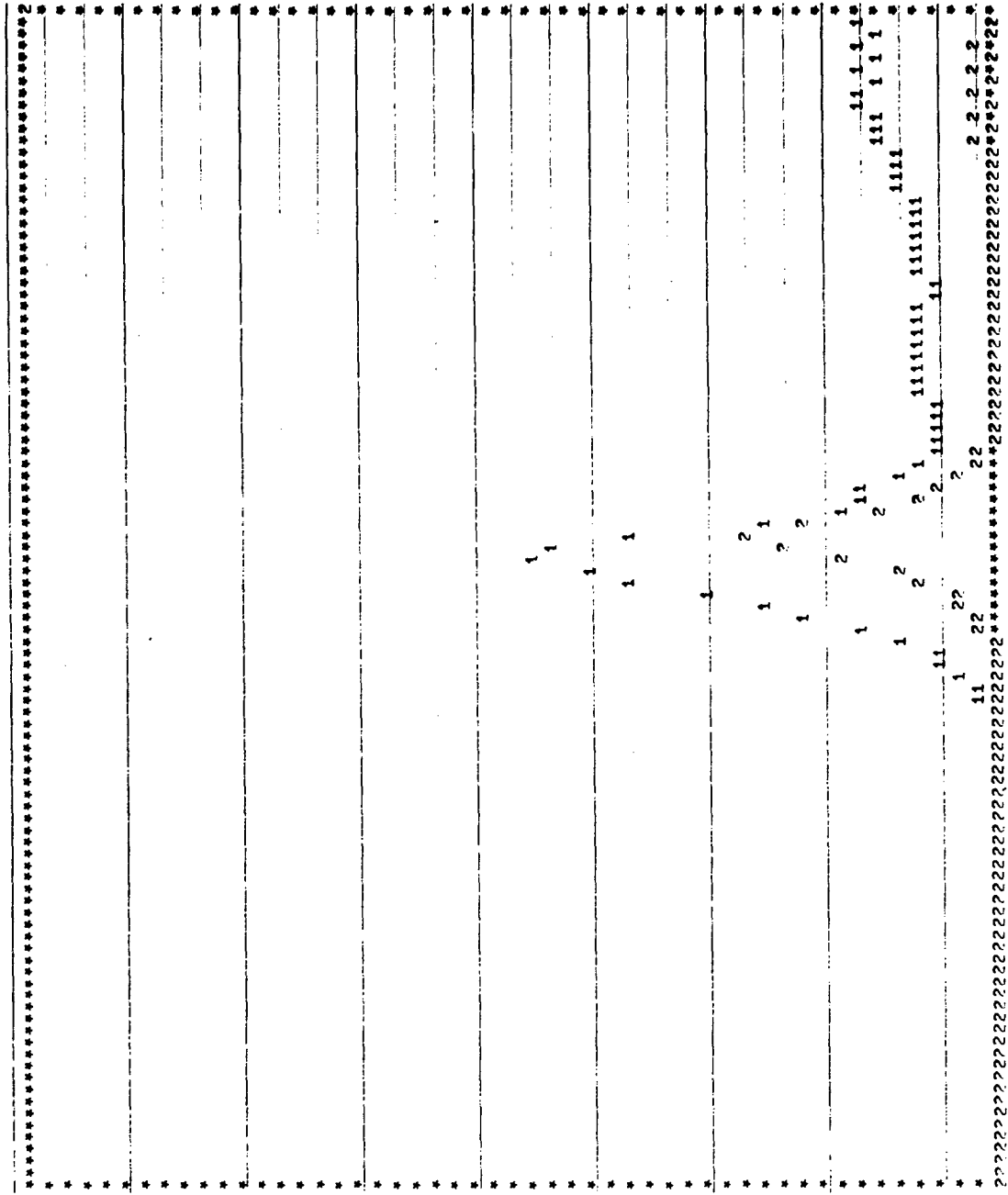


Figure 24. Temperature Behavior (Experiment No. 67) of Ions m/e 50, 51

MASS NO. 66 69
YMAX = .001 .002

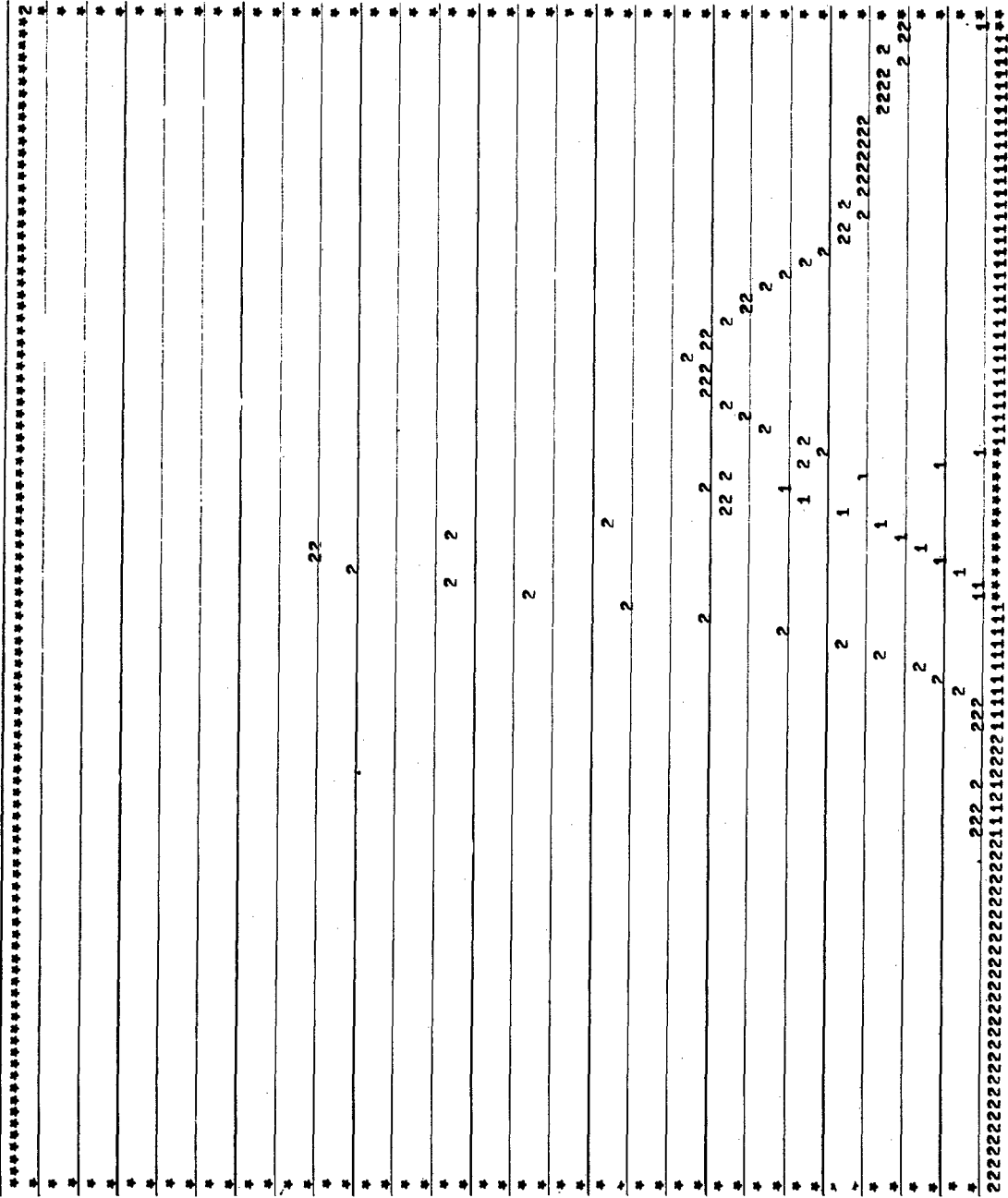
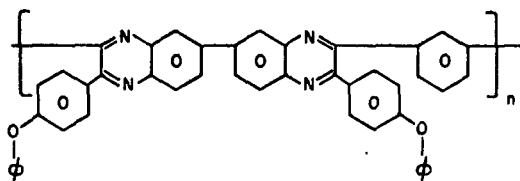


Figure 25. Temperature Behavior (Experiment No. 67) of Ions m/e 66, 69

PPQ4-TS



1. At lowest scans traces of solvent CH_3OH (cf, m/e 31, 32) are present along with background spectrum.
2. Apparent weight loss appears at ~ 200 C. At ~ 350 C, there is evidence of alkyl benzenes (cf, m/e 91, 92); this is probably a mixture of toluene, ethyl benzene, xylene, etc. The intensity of these peaks rises to a maximum at ~ 580 C and then drops.
3. Over the same temperature region (approximately same temperature dependence), benzene (cf, m/e 78, 77, 51, 50, etc.) and phenol (cf, m/e 95, 94, 66, 65, etc.) are formed in approximately equal abundance. The quantity of these maximizes at the same temperature as the region of maximum rate of weight loss.
4. Benzonitrile (cf, m/e 103, 76, 50) begins to evolve at ~ 500 C and achieves a sharp maximum at ~ 600 C and then drops. This is also of abundance similar to benzene and phenol; however, the temperature dependence is quite different. The total release of benzonitrile is over a much narrower temperature range. It appears that there are some other small components at higher mass (some m/e > 190) having a wide range of mass fragments. These all have a very similar temperature behavior to the benzonitrile; however, because of the low intensities, no definitive conclusions can be made.
5. At higher temperatures starting at 600 C, HCN (cf, m/e 27 and m/e ratio 26/27) and apparently N_2 (m/e 28) and/or CO are eliminated achieving a maximum rate of formation at ~ 725 C and then dropping to a minimum at ~ 875 C.

The extent of HCN formation appears to be comparable to the amount of the other major components.

6. There is little or no evidence of appreciable amounts of larger organics that one might expect to be produced (viz, phenetole, benzil, benzaldehyde and phenyl ether, etc.). Absence of phenylacetylene implies structural changes in the polymer at low temperatures.

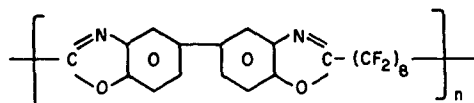
Suggestions for Program Output:

1. Plot $\sum_i I_i$ vs scan number

This should display maxima and minima corresponding to the evolution of the major components. This plot would be comparable to a first-derivative plot of weight loss vs scan number and should be useful in determining the fraction of the weight loss due to volatile components.

2. For best interpretation of the spectral scans, one requires a scale factor for each spectrum. It is easy to see the relative peak intensities; however, it is difficult in comparing scans to tell whether certain peaks are increasing in absolute intensity or all of the others are decreasing. This may involve having a scale factor printed out on the right upper region of the mass spectra.

CD-569-1-31



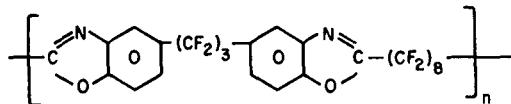
1. There are two major regions of product evolution, viz., 330 C and 530 C. Unfortunately, the weight-loss data have a great deal of scatter, and thus it is difficult to determine where the region of maximum weight loss occurs. Because of the relative peak areas, the region of maximum rate of weight loss will be around 530 C.
2. The low-temperature peak has an onset of 280 C and drops at 380 C. The mass spectra indicate predominantly water with the presence of some other organic species. When water is evolved in large quantities, it displaces molecules from the surfaces which results in mass peaks having no relation to our sample. In this case there are other species released from the sample, but these cannot be identified at present. A comparison with the solvents used in the sample preparation may aid in the identification.
3. Commencing at 460 C, the major gaseous products are evolved. This maximizes at 530 C and is complete at about 600 C. This peak corresponds to perfluorocarbons coming from the $(CF_2)_8$ linkage. Included among these are C_4F_8 (cf, m/e 181, 69, 50, etc.), C_2F_6 (cf, m/e 69, 119, 50, 31, etc.), C_2F_4 (cf, 100, 81 ratio 100/81 = 0.63 [tables]; 0.56 [observed]). In addition, carbon monoxide, water, and F_2 are present. Fluorine appears to be slowly evolved over the whole temperature range; its reactions produce a large HF^+ peak at m/e 20.
4. At slightly higher temperatures (600-800 C), carbon tetrafluoride is evolved (cf, behaviors of m/e 69). Water is also produced in this temperature region.

5. Starting at ~ 670 C, CO, HCN, and H₂O are evolved. These continue to be released up to the highest temperature investigated (~ 900 C).

Suggestions:

1. The polymers which release perfluorocarbons and fluorine tend to disturb the mass spectrometer, resulting in loss of sensitivity and/or resolution. In these cases, it may be necessary to lower the peak detection threshold in order to attempt to pick up other mass peaks. This would be particularly helpful in complex mixtures where isotopic ratios are necessary for identification.

2. A list of solvents or possible impurities submitted along with the sample may be of assistance in clarifying some of the spectra in the lower temperature regions.

96-151

1. The region of rapid weight loss occurs in the temperature region 470-570 C and accounts for about 55% of total.
2. In the plot of total ionization vs scan number, two peaks are apparent, the larger corresponding to the region of maximum rate of weight loss. The absence of intensity at temperatures above ~ 600 C arises from poisoning of surfaces of the instrument. This apparently is due to the release of HF and/or F₂ from the fluorocarbon polymers.
3. In general, only minor differences exist between the spectra for the present sample, as compared to the previous one (CD-569-1-31). The similarity extends from the same species evolved to the decomposition temperatures.
4. At lowest temperatures (300-350 C), HF and organic species are evolved. No water is noted (in contrast to the previous sample). The organic peaks at m/e 28, 43, and 44 appear to be the same as those released in the previous sample. HF was not detected in the previous sample in this temperature region.
5. From 470-570 C evidence for HF, C₂F₄, C₃F₆ is present. No perfluorocarbons with more than three carbons are noted (in contrast to the previous sample detection of perfluorobutane). Appreciable amounts of C₂F₃H and

C_3F_5H are formed as evidenced by the CF_2H^+ peak at m/e 51. These were also detected in the previous sample, although not mentioned in the previous report. The evolution of these fluorocarbon compounds corresponds to the region of maximum rate of weight loss.

6. From 600-800 C carbon tetrafluoride is evolved. This is a broad peak, presumably due to rearrangements required for its formation.

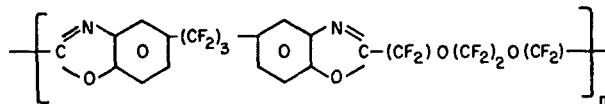
7. At higher temperatures, there is no evidence for H_2O , CO, or HCN elimination as noted in the previous sample.

Suggestions:

1. Plot the first derivative of weight-loss data in cases where the signal-to-noise ratio warrants.
2. Plot on one graph both the first derivative of the weight loss and the total ionization data. This will permit a comparison of rate of weight loss which emphasizes the heavy fragments with the total ionization which emphasizes the lighter volatile samples.

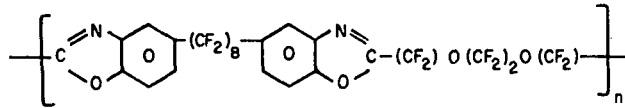
Comments:

1. Lower detection thresholds have been used with some success.
2. Problems with the computer output of the mass-spectra bar graphs have been corrected.



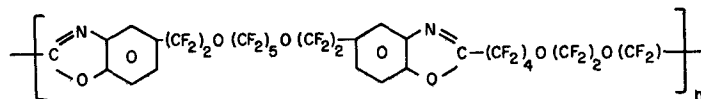
1. Obvious oscillations interfere, but maximum rate of weight loss occurs at ~ 420-480 C.
2. Total-ionization data show several peaks (approximately four); the largest occurs at ~ 460 C.
3. Over the range 30-130 C, water and alkyl benzenes are evolved. Some of this is due to xylene used for filament conditioning.
4. From 290 to 360--exactly as observed for No. 54 (Report IC)-- carbon monoxide and carbon dioxide are evolved as well as some traces of hydrocarbons. The temperature behavior of m/e 44 is unlike any of the other nearby masses, implying that it is CO_2^+ rather than a hydrocarbon peak. Similarly, the identical behavior of m/e 12, 16, and 28 (i.e., C^+ , O^+ , and CO^+) and intensity ratios indicate carbon monoxide.
5. From 420 to 480 C, predominantly carbonyl difluoride (carbon oxyfluoride CF_2O) is evolved. The cracking pattern is very distinctive C^+ , F^+ , CF^+ , CFO^+ , CF_2O^+ . This gas is released over a very narrow temperature range corresponding to decomposition of the ether linkages. In addition, carbon dioxide and hydrogen fluoride are evolved. This sample differs from the previous two in that ether linkages are involved and correspondingly CF_2O is evolved. There is some sign of CF_3OF^+ (m/e 85) being present.

6. Over the latter temperature region around 450 C, there are signs of the perfluorocarbons which dominated in the previous two samples.
7. Starting at 620 C and maximizing at 700 C, carbon tetrafluoride is evolved exactly analogous to the last two samples.
8. From 730 C to the maximum temperature, hydrogen cyanide (cf, m/e 28, 27) is released as in the last two samples.
9. The mass spectra for this sample are the most complex of the present series.

34728-22-1

1. Oscillation prevents interpretation of the weight-loss data.
2. The total ionization curve indicates three peaks not unlike the previous sample.
3. Essentially the spectra and temperature dependence are the same as for the previous sample (cf, Report ID). This is as expected from the minor structural changes in lengthening the CF_2 chain from three to eight units. The only differences revolve around this change. For example, m/e 31 CF^+ which arises both from carbonyl difluoride and perfluorocarbons shows two distinct peaks. This arises from the emphasis on the $(\text{CF}_2)_8$ chain. One would expect a greater relative intensity of perfluorocarbon peaks in this sample. A clear example of this is seen in the ratio $[\text{CF}_3^+]_{\text{max}}/[\text{CFO}^+]_{\text{max}}$ which is 0.4 in this sample and ~ 0.1 in the previous one.
4. Other than these slight differences, the spectra are as in No. 56.

151-85



1. The percentage-weight-loss data indicates that the maximum rate of loss occurs at 510 C. Approximately 70% of the weight loss occurs in the temperature range 510 ± 50 C.

2. The total-ionization curve has an unusual shape due to loss of sensitivity at the higher temperatures. In addition, the summing procedure appears to be in error for this sample because at the region of maximum rate of weight loss, the total ionization is very low.

3. At the lowest temperature (50-200 C), alkyl benzenes are present. Probably xylene used for filament conditioning is the main contributor, along with solvents used for sample preparation.

4. Starting at a very low temperature (150 C), fluorine is produced in abundance. This is the only sample in this series in which this occurs at a low temperature. The evolution of fluorine continues up to ~ 500 C. This seriously deteriorates the mass-spectrometer performance since both loss of sensitivity and discrimination toward the heavier masses occur. Hydrogen fluoride is also produced in small amounts.

5. Carbon dioxide and carbon monoxide are released in the temperature range 150-220 C. In addition there is a separate production of carbon dioxide again over the range 250-420 C.

6. Over the temperature range 426-600 C, carbonyl difluoride (CF_2O) is produced in three distinct maxima. These apparently arise from the different locations of the ether linkages in the polymer. The same structure appears in all the fragments C^+ , O^+ , CF^+ , CFO^+ as well as the molecular ion. In addition, a mass 85 peak is also noted in the last two samples, apparently due to CF_3OF , although no mass spectrum is available for comparison.

7. Over the latter part of this temperature region, the larger perfluorocarbons are released (cf, mass 119, 100, 50, etc.). This is analogous to the last two samples. The evolution of these perfluorocarbons and carbonyl difluoride corresponds to the region of maximum rate of weight loss.

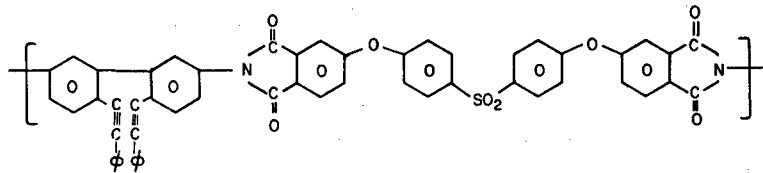
8. Analogous to all of the samples in this series, carbon tetrafluoride CF_4 is produced in the temperature range 570-870 C, maximizing at 670 C.

9. At the maximum temperature, hydrogen cyanide and carbon monoxide are released as in the previous samples.

10. The major difference in the final sample is the release of fluorine at the low temperatures (start of weight loss), although the maximum rate of sample decomposition corresponds to elimination of the perfluorocarbons and carbonyl difluoride.

Suggestion:

1. The possibility of using lower electron energies to eliminate many fragment ions may elucidate the mass spectra in cases where most of the gases are released in a narrow temperature region.

FLH-PI4

1. The weight-loss data display very little of the scatter which is characteristic of some of the previous runs. Two regions of apparent weight loss exist at 190 C and at 540 C. The region of maximum rate of weight loss occurs at 550 ± 100 C; this region accounts for about 50% of the total weight lost.

2. In the total-ionization curve two major peaks are evident, one at 105 C and the other at 550 C. The latter, being the larger, corresponds to the region of maximum rate of weight loss.

3. From 50 to 150 C, dimethyl acetamide mass peaks are present (cf, m/e 44, 43, 15, 87, 42, etc.). This is apparently trapped solvent being released. In addition, water is eliminated gradually over the whole temperature range of the experiment. There is some evidence for C_2 species such as ethane, but there is considerable interference from the dimethyl-acetamide peaks.

4. Methanol is released over the temperature range $100 \rightarrow 220$ C (cf, m/e 31, 32, 29).

5. Over the same temperature interval 400-600 C, a larger number of species is evolved. Their evolution corresponds to breaking C-O and C-S bonds in the polymer. This is summarized as follows:

- a. Sulfur Dioxide: maximum rate of evolution at 510 C.

- b. Phenol: two maxima--one at 510 C and one at 570 C--are observed. The former is consistent with SO₂ production in which C-S bonds are broken and phenol would be the next logical species to be released. The second temperature maximum may correspond to releasing phenol from a different environment in the polymer.
- c. Carbon Monoxide: maximizes at 610 C.
- d. Carbon Dioxide: (530-630 C) with a maximum at ~ 570 C.
- e. Benzene: exactly same temperature dependence as CO₂.

6. At higher temperatures and in certain intermediate temperature ranges, there is evidence for some release of gases from the previous sample. For example, perfluorocarbon peaks (m/e 19, 31, 69) are present in small amounts.

Suggestions:

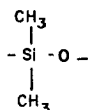
From previous discussions in which it was concluded that the most useful information arises from the lower temperature regions, it is apparent that in these temperature regions, solvents and mass-spectrometric background peaks cause serious problems in the detection of the initial polymer breakdown. It would appear helpful to determine the temperature regions in which the first gases are evolved. Then, a separate sample could be pre-treated by heating to this temperature to completely drive off the solvents. A preliminary test could be used to determine whether the polymer has degraded and whether it should be resubmitted for a second mass-spectrometric analysis in which a careful analysis of the low-temperature gas evolution could be conducted. In this way the relative importance of the first detected gases could be ascertained.

1. In the weight-loss curve in the very low-temperature region, there appears to be some computer format error; however, the basic features are clear. The majority of the weight loss (~ 50%) occurs in the temperature region 580 ± 70 C.

2. The total-ionization behavior over the temperature range of the experiment is shown. Only one major peak is present, corresponding to the temperature of the maximum rate of weight loss.

3. Trimethyl silanol $(\text{CH}_3)_3\text{SiOH}$, as evidenced by m/e 45, 75, is evolved over the temperature range 280-450 C, with a maximum at 380 C. The quantity is very small and therefore not apparent on the total-ionization curve.

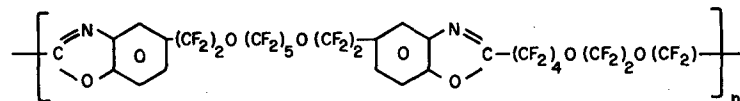
4. The major degradation occurs over a broad temperature range 380-720 C, with a maximum at 580 C. Water and alkyl siloxanes are evolved. The former appears as m/e 17, 18 having the same temperature dependence as the siloxane. The mass spectrum at $T = 580$ C is shown. The highest mass observed--281--corresponds to $(\text{CH}_3)_7\text{Si}_4\text{O}_4^+$. The repeating structure in siloxanes (silicones) is



having mass 74. All of the major higher mass peaks--m/e 45, 59, 73, 133, 147, 207, and 281--are characteristic of siloxanes. For example, m/e 207 corresponds to loss of Si_2O , m/e 147 corresponds to a further loss of CH_5SiO , etc. No attempt has been made to identify the precise structure

of the silicone. A typical example of a linear silicone is $[\text{SiR}_3 - \text{O} - \text{SiR}_2 - \text{O} - \text{SiR}_3]$; when $\text{R} = \text{CH}_3$, this is octamethyl trisiloxane.

5. The masses 12, 13, 14, 15, and 16 all appear to have two temperature maxima. The first corresponds to silicone fragments, and the higher temperature maximum at $\sim 690 \text{ C}$ corresponds to methane evolution.

151-85

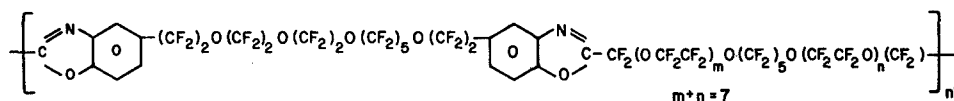
1. From the weight-loss curve it is evident that 50% of the weight is lost in the temperature interval 520 ± 50 C. The extra points arising from computer error in the previous run (Report IF) have been corrected.
2. The total-ionization behavior indicates maxima at 460 and 560 C.
3. Starting at 110 C and maximizing at ~ 460 C, fluorine is evolved. This is evident from the behavior of m/e 19 (F^+). The maximum occurring at 520 C apparently is correlated with a competition in which carbonyl difluoride, hydrogen fluoride, and the perfluorocarbons are preferentially evolved.
4. Carbon monoxide and carbon dioxide are produced as reported previously. The latter passes through three successive maxima, two of which correspond to the temperatures for production of carbonyl difluoride.
5. Carbonyl-difluoride production maximizes at 480 C and 575 C, apparently due to different environments in the polymer. In the previous run of this sample, a third maximum was observed. In addition, the m/e 85 peak attributed to CF_3O^+ is present (three maxima), and different behavior to that of carbonyl difluoride is exhibited.
6. From 540 to 580 C a large number of perfluorocarbons is released. The following ions are observed: CF_3^+ , $C_2F_3^+$, $C_2F_4^+$, $C_2F_5^+$ (from C_2F_6 and C_3 species), $C_3F_7^+$, and $C_4F_7^+$. In addition at slightly higher temperatures, carbon tetrafluoride is evolved.

7. Interestingly, CF_2^+ (m/e 50) and C_2F_4^+ (m/e 100) are accompanied by CF_2H^+ (m/e 51) and $\text{C}_2\text{F}_4\text{H}^+$ (m/e 101) in almost equal abundances.

8. Overall, a rerun of this sample has resulted in considerably more sensitivity of product detection. The temperature behavior of fluorine was reproduced; however, some of its deleterious effects were less pronounced in this run.

9. Considering the number of ether linkages, it is surprising that perfluorocarbon fragments $(\text{CF}_2)_n^+$ are present in such abundance.

210-51

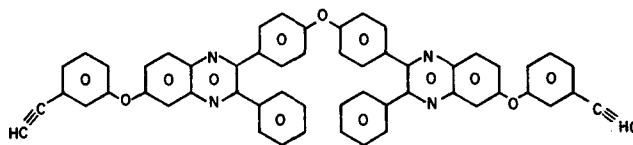


1. The percentage weight loss indicates maximum rate of change at temperature 510 C, with ~ 50% weight loss in the range ± 50 C. First-derivative plots would show several maxima.
2. The total-ionization behavior displays two distinct maxima at 500 C and 570 C, the latter being much narrower. In addition, there is a long rising tail at the highest temperatures.
3. Starting at 150 C fluorine is eliminated, achieving a maximum rate of formation at 500 C, followed by a very sharply declining rate minimizing at 570 C. As the temperature is raised, further fluorine is produced in high abundance. As noted in the previous reports, this sudden minimum which occurs precisely at the temperature of maximum rate of evolution of the perfluorocarbons appears to arise from a competition between loss of F_2 or $(\text{CF}_2)_n$. The latter dominates in a narrow temperature region in which simple-bond cleavage occurs faster than the rearrangement mechanism required in fluorine production.
4. Carbon dioxide--as in previous analogous samples--appears to be evolved in the same temperature regions as carbonyl difluoride. CO_2 production starts at ~ 190 C and reaches a maximum at ~ 500 C and then declines. This is over a broad temperature range. A second very narrow maximum occurs at 570 C in conjunction with the release of carbonyl difluoride.

5. Two distinct regions of maximum evolution of carbonyl difluoride (CF_2O) exist at 500 and 570 C, consistent with the total-ionization maxima. Some related oxyfluorocarbon species CF_3O^+ and CF_3CO^+ are detected which have very similar temperature behavior to CF_2O . These may be fragments of the fluorocarbon analogues of methanol and acetaldehyde.

6. At 570 C a whole range of perfluorocarbons is observed to have a maximum rate of formation. Fragments ranging from CF_2^+ to C_4F_9^+ are detected. Along with CF_3^+ and C_2F_5^+ the partially fluorinated species CF_2H^+ and $\text{C}_2\text{F}_4\text{H}^+$ are observed. Similar temperature behavior exists for CF_3^+ from carbon tetrafluoride and C_2F_5^+ from perfluoroethane.

7. At higher temperatures the large number of fragment ions increases sharply. An estimate of the species evolved can be made. CF_2O , HF, and perfluorocarbons whose formation does not require a molecular rearrangement (e.g., C_2F_4 but not C_2F_6) are eliminated.

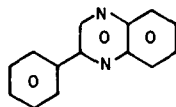


1. The maximum rate of weight loss occurs at 550 C with at least 50% lost within the interval ± 50 C.
2. The first-derivative plot of the weight loss displays a maximum in the range 530-550 C. Of the numerous other peaks apparent, none appears to correspond to legitimate weight loss. These spurious peaks arise from excessive noise in the weight-loss curve.
3. Interestingly, the maximum in the total-ionization curve occurs in the vicinity of 500-580 C which is slightly higher than the region of the maximum in the first-derivative curve. This may indicate evolution of nonvolatile fragments which have little opportunity to reach the ionization region. The latter emphasizes the higher-molecular-weight species, whereas the former emphasizes the lower-molecular-weight volatile species.
4. In general, all of the products are detected in a very narrow region of temperature--460 \rightarrow 660 C. In cases where all of the products have a similar temperature dependence, it is difficult to make precise identification of all of the products evolved.
5. Within the temperature profile for product formation, slight differences are apparent. For example, the first volatile fragments detected are alkyl benzenes. The tropylium ion $C_7H_7^+$ indicates their temperature behavior. The ratio of m/e 92/91 suggests that toluene may be the major component; however, all of the alkyl benzenes have similar ratios.
6. At slightly higher temperatures ($\Delta T \sim 50$ C), benzene, phenol, and water are eliminated. The water can be identified only by the ratio m/e 19/18 which is not consistent with the presence of carbon. With the exception of water, some of these species approach the amount of alkyl benzene evolved.
7. Benzonitrile is also detected (cf, m/e 103).

8. A very intense m/e 28 peak is observed. No carbon dioxide is produced, and the isotopic ratios of the neighboring masses are not consistent with hydrocarbon fragments $C_2H_3^+$, $C_2H_4^+$. It appears that this peak corresponds to CO^+ from carbon monoxide.

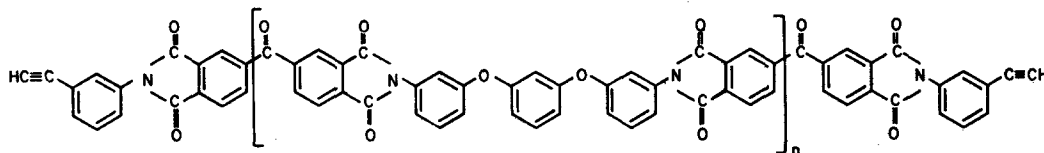
9. At somewhat higher temperatures (~ 730 C), there is evidence for hydrogen-cyanide (HCN) production (cf, m/e 26, 27) during the cracking of the stable aromatic rings.

10. Some higher-molecular-weight ions are observed, but since their abundance is very low, no definite conclusions can be reached. However, a low-intensity ion at m/e 206 may correspond to



Comments:

It appears that the first-derivative plots will be very useful. In order to best utilize the available information, the behavior of the output from the electrobalance must be improved. It is not clear whether the drop in the weight loss at the highest temperatures is a legitimate experimental observation or an instrumental artifact.

HR 600

1. The percent weight loss indicates that 75% of the sample weight is lost in the interval 560 ± 90 C. Unusual behavior occurs above the region of weight loss, indicating weight gain; the cause should be investigated.

2. The total-ionization current maximizes at a slightly higher temperature-- 600 C-- than the region of maximum rate of weight loss. In addition, a solvent peak maximizing at 180 C is apparent. In the corrected total-ionization curve, the maximum is shifted to lower temperature. The slight wings noted arise from the saturation of the output for m/e 28.

3. There are various computer difficulties plaguing the output. Most of these have been present for some time but have been overlooked. The following is a partial list:

- a. m/e 1 is not real.
- b. m/e 7 is listed with a negative intensity, yet only about four temperature scans wide.
- c) m/e 28 is the largest peak observed and overshoots the computer intensity range. This results in adding an incorrect ion intensity in the overflow region. In the present case, this seriously upsets the total-ionization curve and creates very confusing mass spectra. This may, in fact, account for the displacement of the total-ionization maximum. This is now corrected and another decade of intensity can be recorded.

4. Various solvents are detected in the temperature region 90-220 C (maximum at ~ 180 C)

- water
- ethanol
- cresol (the ratio 107/108 suggests that this may be para cresol)
- an m/e 28 peak is present in this region and may be attributed to CO; however, this can only be considered tentative.

5. The major volatile gases produced are carbon monoxide and carbon dioxide. The ratio $\text{CO}^+/\text{CO}_2^+$ at maximum evolution is ~ 2.1/1. These gases dominate the spectra to such an extent that the fragment O^+ is larger than many of the other species involved (440-790 C maximum at 600 C).

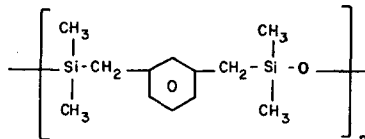
6. In roughly the same temperature region, traces of benzene, alkyl benzenes (toluene), phenol, and benzonitrile [cf, m/e 103; this was erroneously assigned to phenyl acetylene (m/e 102) in Report IIB] were found.

7. At slightly higher temperature (~ 630 C), hydrogen cyanide is evolved at a maximum rate.

8. There is good spectral intensity in the temperature region of the curing reaction; therefore, a closer investigation may yield further identification of volatile species.

9. A large number of peaks are present at higher m/e ratios. Because of the very low intensities relative to the volatile species discussed above, no attempt was made to identify these. Their intensities are roughly 10^2 less than CO^+ at the region of maximum rate of weight loss.

EWC-56-391-2A



1. The weight loss indicates a fairly narrow temperature range of decomposition. Approximately 70% of the sample is lost in the interval 565 ± 30 C.

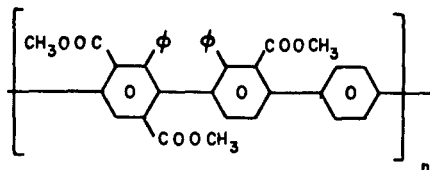
2. Peaks at m/e 221, 207, and 193 indicate silicone products evolved accompanied by loss of $(\text{CH}_2)_n$, where $n = 1, 2, 3$ from the monomer molecular weight of 236.

3. In addition, a homologous series of species containing carbon is observed. For example, m/e 73, 59, and 45 correspond to $\text{Si}(\text{CH}_3)_3^+$, $\text{SiH}(\text{CH}_3)_2^+$, and $\text{SiH}_2\text{CH}_3^+$.

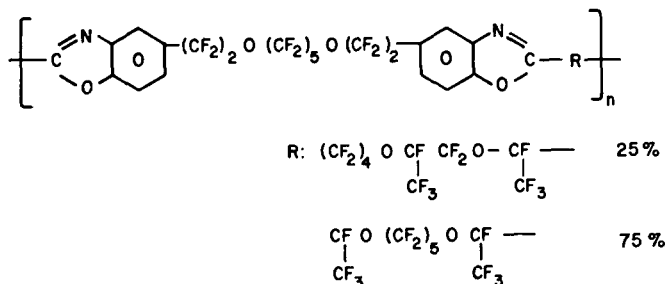
4. Lesser amounts of alkyl benzenes (cf, m/e 91) and benzene (cf, m/e 78, 77, 50, 51, etc.) are detected.

5. Ions corresponding to fragments of C_2 and C_3 hydrocarbon (cf, m/e 27, 28, 29, 41, and 43) are observed in the region at 570 C and also at higher temperatures (~ 640 C).

Report IIE-75



1. The weight-loss data indicate a more gradual weight loss than occurs with the fluorocarbon elastomers. Approximately 30% is lost in the interval 520 ± 50 C.
2. The first derivative of the weight loss indicates sample weight loss at 390, 500, and 620-680 C.
3. The total-ionization behavior shows only one major region of gaseous product evolution at ~ 510 C.
4. The ion sensitivity in this experiment was much below the normal operating level, thus hampering the detection and identification of minor products of the decomposition. This is the case for the products released in the vicinity of 390 C. Low-intensity peaks at m/e 26, 27, 35, 36, and 38 cannot be ascribed to a definite product.
5. The major gaseous products are all detected in the same temperature region ($\sim 520 \pm 30$ C). The FWHM of these species is $\sim 30-40$ C. Carbon monoxide, carbon dioxide, and benzene are the major products. Methanol is released in lesser abundance. No C_2 hydrocarbons are evolved (negligible m/e 27); however, there are very large ions at m/e 29 and 30, corresponding to HCO^+ and H_2CO^+ , possibly from formaldehyde. There is considerable overlap of fragment ions so that a computer analysis for best spectral fit would be informative. Certainly CO , H_2CO , CO_2 , and C_6H_6 are not inconsistent with the observed intensities.
6. From 620-680 C a large amount of methane is evolved which does not show up clearly because of the relatively low total-ionization cross section of methane compared with that of other major products.



1. From the percent-weight-loss curve, ~ 75% of the sample weight is lost in the interval 500 ± 50 C. The rate of loss is very rapid, as shown by the first-derivative plot. The FWHM of the main peak is only ~ 50 C°.
2. Total-ionization behavior indicates three major temperature regions of gaseous product evolution. These have maxima at 285 C, 500 C, and ~ 980 C.
3. As with the previous samples which evolve large amounts of F₂, the sensitivity is quite low; however, identification of the major evolved gases is possible.
4. The major gas evolved is F₂. The rate of production closely follows the total-ionization curve, displaying two distinct maxima and a tailing upwards of the highest temperatures achieved.
5. There is a close parallel with 151-85, cf, MTA No. 58, No. 62. In each case the F₂ production turns down suddenly when the other major products are released. For example, the carbonyl difluoride, carbon dioxide, carbon monoxide, and perfluorocarbon evolution maximizes at ~ 520 C--a temperature at which the F₂ production has dropped by ~ 30%. This apparently reflects a competition between F₂ elimination and other bond cleavages. The activation energy for F₂ production is certainly lower; however, the slower rearrangement process required in its production cannot compete effectively with faster simple-bond cleavage.

6. Carbonyl difluoride production maximizes at ~ 520 C and again at 570 C, indicating two distinct maxima as noted in 210-51 and 151-85 presumably arising from two different environments in the polymer.

7. Carbon monoxide is produced quite abundantly. The intensity as a function of temperature is asymmetric. Carbon dioxide displays the same behavior. Both CO and CO₂ evolution have a broader temperature dependence than CF₂O. However, as noted in previous reports on samples of this type, CF₂O production is frequently accompanied by CO₂ production. In this case, CO₂ behavior is related to the lower-temperature release of CF₂O.

8. Other perfluorocarbons are produced in the vicinity of 520 C, although no ions larger than C₂F₄⁺ were observed because of the low sensitivity.

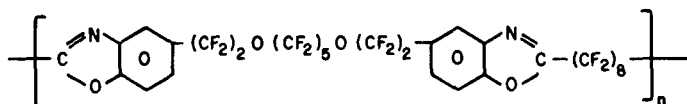
9. Carbon tetrafluoride--as in all of these samples--has a broad temperature evolution maximizing around 680 C.

10. As noted in some previous samples, the ions m/e 50 and 51, i.e., CF₂⁺ and CF₂H⁺, have slightly different temperature dependences and interestingly both ions are of similar abundance.

11. At the highest temperatures, F₂, HF, and CO are evolved. Hydrogen fluoride also has a maximum rate of formation around 570 C (corresponding to CF₂O evolution).

12. No signs of S or any fragments from ethyl mercaptan were detected at the present levels of sensitivity.

95-151



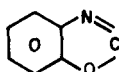
1. From the percentage-weight-loss curve, 50% of the sample weight is lost over the temperature range 530 ± 50 C. This is a much slower decomposition than 91-210 in which there are ether linkages in each of the long chains.

2. FWHM of the total-ionization curve is ~ 60 C°.

3. Large amounts of fluorine are evolved, maximizing at 280 and 530 C followed by a third maximum at the highest temperature studied. Again, the minimum above 530 C appears to arise from competition from the other fragmentation routes.

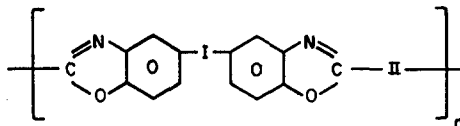
4. Hydrogen fluoride is evolved over a narrow temperature range maximizing at 540 C.

5. Carbon dioxide and carbon monoxide are produced in abundance at 540 C. Apparently the origin of the C and O is not the ether linkages but rather the heterocyclic



In most of the previous samples in which CF_2O was evolved, CO_2 usually displayed a very similar temperature dependence to the CF_2O . This sample is in marked contrast.

6. Carbonyl-difluoride production maximizes at 560 C (only one maximum). For the general formula



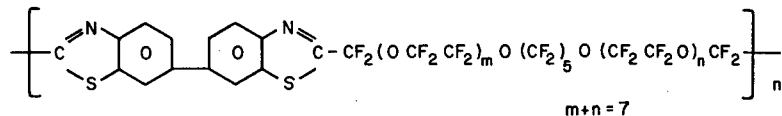
ethers located at I are more stable than those located at II. When ethers are present in both locations, CF_2O displays two distinct maxima separated by as much as 90 C° . The following table is a brief summary of the pertinent information.

Report No	MTA No.	Sample Number	Ether Locations	Number of CF_2O Peaks	Temp. at Maximum Rate of Evolution	
ID	56	151-80	II	1	~ 450	
IE	57	34738-22-1	II	1	~ 450	
II	62	151-85	I II	2	~ 480	~ 575
IIA	63	210-51	I II	2	~ 500	~ 570
IIF	67	91-210	I II	2	~ 520	~ 570
IIG	68	95-151	I	1	~ 560	

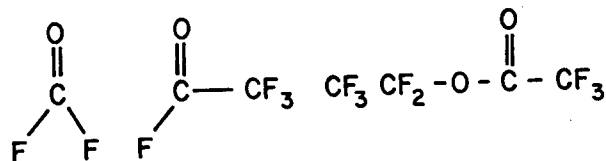
7. The perfluorocarbon peaks maximize around 540 C . A comparison of CFO^+ from CF_2O with CF_2^+ shows two different temperature dependences. In addition, the broad hump in CF_2^+ at higher temperatures arises from CF_4 , whereas the main maxima arise from larger perfluorocarbons.

8. Interestingly, CF_2H^+ is a very large peak--even larger than CF_2^+ or CF_3^+ . In this as well as in most of the previous samples, some interesting H substitution effects are present which may warrant closer scrutiny.

9. A peak at m/e 85 is present which has previously been ascribed to CF_3O^+ . This maximizes at ~ 540 C.
10. There are traces of benzene and other higher molecular species present which cannot be directly assigned.
11. At the highest temperatures, F_2 and CO are evolved.



1. Only one major temperature region of volatile sample evolution is apparent in the weight-loss and total-ionization curves.
2. Fluorine--as in many of the samples in this series--is a major product. Its production reaches a maximum at 460 C.
3. A series of ion fragments from the ether decomposition is observed. This includes CFO^+ , CF_2O^+ , CF_3O^+ , $\text{C}_2\text{F}_3\text{O}^+$, and $\text{C}_4\text{F}_6\text{O}_2^+$. The latter two masses--97 and 213--were observed in MTA No. 63 but were not assigned. It is apparent that these arise from the fluorocarbon analogues of aldehydes and esters.

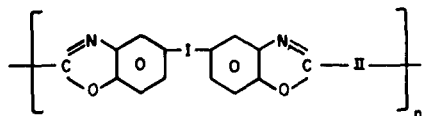


The m/e 47 peak-- CFO^+ --is probably the major fragment of all of these species analogous to CHO^+ .

4. The temperature profile of CFO^+ and CF_2^+ can be compared. The latter onset is lower and the peak is broader. This is a clear indication of the different chemistry involved in their production.
5. CO^+ and CO_2^+ are produced in the same temperature region as CF_2O .
6. There are many more fragment ions from the higher perfluorocarbon, cf, C_2F_4^+ , C_2F_5^+ , C_3F_5^+ , C_4F_9^+ --in particular, C_2F_5^+ .
7. Aside from a slight indication of S (m/e 32), there are no indications of any of the heterocyclics among the volatile species.
8. The maximum ratio of CFO^+ occurs at 490 C; this is in excellent agreement with the location of the ether linkage (cf, Report IIC, Table).

D. FLUOROCARBON ELASTOMER SERIES

Nine of the samples analyzed during this reporting period fall into the category of fluorocarbon elastomers. Their molecular formula can be represented by the schematic structure



where I and II represent various fluorocarbon or fluoroether chains summarized in Table 3.

In the following analysis it is assumed that the two locations I and II are unique and that there is a statistical representation of fluorocarbon and fluoroether chains. However, the set of samples analyzed is not a complete one in which every chain has been substituted in each location. For example, all of the ethers substituted in Position I have $O-(CF_2)_2^-$ as the last element, whereas all of the ethers substituted in Position II have $O-CF_2^-$ as the last element. Further samples must be analyzed to determine whether chain structure or chain location determines the stability.

1. I and II Represent Fluorocarbons

Two samples, CD-569-1-31 (Experiment No. 54) and 96-151 (Experiment No. 55), fall into this category. Table 4 summarizes pertinent temperature data. The ions CF_2^+ and CF_3^+ are representative of perfluorocarbon products formed directly by degradation of the polymer. Although F^+ is also a fragment ion of these species, its magnitude implies that it arises primarily from fluorine (F_2) production. Independent of the location (I or II) of (CF_2)

TABLE 3
FLUOROCARBON FORMULAE

Sample	I	II
CD-569-1-31	nil	$-(CF_2)_8^-$
96-151	$-(CF_2)_3^-$	$-(CF_2)_8^-$
95-151	$(CF_2)_2 O-(CF_2)_5 -O-(CF_2)_2$	$-(CF_2)_8^-$
151-80	$-(CF_2)_3^-$	$-CF_2-O-(CF_2)_2 -OCF_2^-$
34728-22-1	$-(CF_2)_8^-$	$-CF_2-O-(CF_2)_2 -OCF_2^-$
55584-20 ^a	nil	$CF_2-(OCF_2 CF_2)_m -O-(CF_2)_5 -O(CF_2 CF_2 O)_n -CF_2^-$ $m+n=7$
151-85	$-(CF_2)_2 -O-(CF_2)_5 -O-(CF_2)_2$	$(CF_2)_4 -O-(CF_2)_2 -OCF_2^-$
210-51	$(-CF_2 CF_2 O)_3 (CF_2)_3 -O-(CF_2)_2$	$CF_2(-OCF_2 CF_2)_m O(CF_2)_5 -O(CF_2 CF_2 O)_n CF_2^-$ $m+n=7$
91-210	$-(CF_2)_2 -O-(CF_2)_5 -O-(CF_2)_2$	25% $-(CF_2)_4 -OCF_2 CF_2 O-CF_3$ 75% $-CF-O-(CF_2)_5 -O-CF-CF_3$

^a Benzothiazole.

chains within the polymer, the maximum rate of fragmentation occurs in the interval 530 ± 10 C. This corresponds to breaking $\text{CF}_2\text{-CF}_2$ bonds. Fluorine production does not involve simple bond cleavage but rather a rearrangement process in which the F-F bond is forming as the C-F bonds are breaking in a concerted reaction.

TABLE 4
TEMPERATURES OF SAMPLE EVOLUTION: FLUOROCARBONS

Sample	<u>Temperature (maximum rate of formation)</u>				
	I	II	CF_2^+	CF_3^+	F^+
CD-569-1-31	—	$(\text{CF}_2)_8$	540	530	540
96-151	$(\text{CF}_2)_3$	$(\text{CF}_2)_8$	520	535	520

2. Fluoroethers Inserted

Nine samples fall into this category. Table 5 summarizes representative data. CFO^+ is assumed to be representative of the behavior of the series of oxyfluorocarbons formed by decomposition of the ether chains. Although CO^+ is a fragment ion of this species, its high abundance implies that it is more representative of carbon-monoxide formation.

a. Primary Effects

Three different situations exist regarding temperature of the maximum rate of formation of CFO^+ . Presumably CFO^+ appearance indicates bond cleavages within the ether chain(s). When the ether chain is located in Position I, the temperature at maximum ether fragmentation is 570 ± 10 C (95-151); in Position II the corresponding temperature is 480 ± 10 C (151-80, 34738-22-1, 55584-20); finally, when ethers are present in both locations, one maximum is present at 575 ± 10 C and another at 510 ± 20 C. This effect may be related to the different chemical environments at these two locations. The increased stability of the ether chain located adjacent to the six-membered rings may be associated with interactions of the π -electrons of the stable ring with fluorine or oxygen.

TABLE 5
TEMPERATURE OF SAMPLE EVOLUTION: FLUOROETHERS

Sample	Ether Locations		Temperature (C); maximum rate of formation					
	I	II	CF ₂	CF ₃ ⁺ CO ⁺	CO ₂ ⁺	CFO ⁺	F ⁺	
95-151	-(CF ₂) ₂ O (CF ₂) ₅ O (CF ₂) ₂ -	-(CF ₂) ₈ -	550	555 550	550	570	535	
151-80	-(CF ₂) ₃ -	-(CF ₂) ₂ O (CF ₂) ₂ O (CF ₂) ₂ -	485	---	485	485	485	
34728-22-1	-(CF ₂) ₈ -	-(CF ₂) ₂ O (CF ₂) ₂ O (CF ₂) ₂ -	480; 560	---	470	470	480	
55584-20		-(CF ₂) ₂ O (CF ₂) ₂ O (CF ₂) ₅ O (CF ₂) ₂ O (CF ₂) ₂ -	480	490 480	470	490	450	
151-85	-(CF ₂) ₂ O (CF ₂) ₅ O (CF ₂) ₂ -	-(CF ₂) ₄ O (CF ₂) ₂ O (CF ₂) ₂ -	570	570 460; 570	480; 550	500; 570	475	
210-51	-(CF ₂) ₂ O (CF ₂) ₂ O (CF ₂) ₂ O (CF ₂) ₅ O (CF ₂) ₂ -	-(CF ₂) ₂ O (CF ₂) ₂ O (CF ₂) ₂ O (CF ₂) ₂ O (CF ₂) ₂ -	570	570 500; 570	500; 570	500; 570	510	
91-210	-(CF ₂) ₂ O (CF ₂) ₅ O (CF ₂) ₂ -	R: (CF ₂) ₄ O CF ₃ CF ₂ O-CF ₃ --- 25% CF ₃	520	525 540	535	530; 580	495	
		CF ₃ O (CF ₂) ₅ O CF ₃ --- 75% CF ₃						

b. Secondary Effects

Both CO^+ and CO_2^+ production accompany the ether decomposition. Similarly, fluorine production is intimately related to the ether decomposition. In fact, there is strong evidence in these samples of competition effects between F^+ and CFO^+ . As mentioned earlier, fluorine production requires an extensive rearrangement. These fragmentation processes usually have lower activation energies than simple bond cleavages because of their concerted nature; however, their rates are slower-rising functions of energy. Thus, they are very competitive at the lower temperatures but much less competitive with bond cleavage processes which have a higher activation energy yet a rate that increases more rapidly with energy. In many of these samples, F^+ production maximizes at a fairly low temperature but passes through a minimum at the temperature region where CFO^+ and CF_3^+ production maximizes.

3. Carbon Tetrafluoride Formation

Another interesting correlation -- not shown in Figures III and IV -- involves CF_3^+ production. With only one exception (55584-20), in which S is substituted for O in the heterocyclic portion, carbon tetrafluoride (CF_4) is formed at higher temperatures. Once again this involves a rearrangement and it is manifested in a second CF_3^+ peak with a broad rate of production at higher temperatures. For these samples this rate maximizes in the range 680 ± 20 C. This is of considerably less interest because most of the chemistry associated with primary fragmentation of the polymer has occurred at temperatures below 600 C. It appears that CF_4 is not a primary product but rather a secondary decomposition fragment of a fairly stable, nonvolatile intermediate. Hence, its temperature behavior is almost independent of the initial polymer structure.

4. Analysis of Threshold Temperatures

Because of the interesting stability effects related to chain composition or location within the polymer, it is worthwhile to look at these data more carefully. From a thermochemical vantage point, the onset temperature of a particular reaction is of considerable importance. It is rather difficult to determine a precise onset temperature for several reasons:

First -- with the exception of threshold functions that are linear or step functions -- the definition of an onset region is rather arbitrary. Secondly, an arbitrary threshold exists below which the computer program rejects an ion peak. One technique commonly used in mass spectrometry for ion-appearance-potential estimates is the semi-logarithmic method of extrapolation developed by Lossing.⁵ Thirdly, no justification can be given for applying this particular threshold-determination technique; however, an attempt has been made to extrapolate the ion profiles for CFO^+ to obtain an approximate onset, analogous to the vanishing current technique. With these reservations, the temperature onsets are listed in Table 6 along with the temperature at maximum rate of formation. Two onset values are listed for Sample 55584-20 which has the sulfur substitution. It is not obvious why this polymer should fit into this series; however, two onsets were apparent and are listed for completeness. To summarize, when the ether is located in Position I but not in II, the temperatures at the onset and at the maximum rate of CFO^+ production are ~ 450 and ~ 570 C, respectively. When an ether is located in Position II, the corresponding temperatures are 360 (average) and 550 ± 30 C. Certainly the onset temperatures reflect only the lower-energy process and as pointed out earlier, this process is the fragmentation of the ether linkage at Position II.

The threshold-temperature data is consistent with the temperature at maximum rate of formation. There is a difference of 80-100 Centigrade degrees in the two ether decompositions. This may, in fact, reflect differences in the stability of the two locations within the polymer or possibly a difference in the structure of the ether chains. This can be readily resolved by the analysis of an ether of the form $-\text{CF}_2-\text{O}-(\text{CF}_2)_2-\text{O}-(\text{CF}_2)-$ in Position II. If stability is related to the chain environment, CFO^+ production will maximize in the region 480 ± 40 C. If the stability is related to chain structure, CFO^+ production will maximize in the region 580 ± 20 C.

TABLE 6
ONSET TEMPERATURE FOR ETHER FRAGMENTATION

<u>Sample</u>	<u>Ether Location</u> ^a		<u>Temperature (C); CFO⁺</u>	
	<u>I</u>	<u>II</u>	<u>Onset (estimate)</u>	<u>Maximum Rate</u>
95-151	✓	-	450	570
151-80	-	✓	380	485
34728-22-1	-	✓	350	470
55584-20	-	✓	270;360	490
151-85	✓	✓	340	500;590
210-51	✓	✓	330	500;590
91-210	✓	✓	375	530;580

^aSee Table 5 for structures.

SECTION IV

FUTURE PLANS

Attention¹ has been focused on the need for absolute pressure determination to quantify the amounts of volatile products evolved. The practicability of absolute calibration can be better evaluated at the completion of the extensive vacuum modifications now underway. Since adequate tabulations of total ionization cross sections are available,^{6,7} strong consideration will be given to their use in quantifying relative intensities. Furthermore, the displayed additivity of total ionization cross sections in homologous series may be particularly useful with polymers.

Currently, a data bank of mass spectra has been compiled. Methods of selecting subsets relevant to particular polymer systems are being pursued. Eventually, the operator will be able to select the appropriate mass spectral subset by simply answering a series of simple questions concerning the sample. This subset will then be available for utilization in conjunction with the computer search and analysis program.³

Efficiency of the modified vacuum system will determine whether a GC-MS coupling in the present instrument is feasible. With the current data-handling capability, the modification required to the mass spectrometer would be rather minimal. Such a GC-MS capability would greatly augment the present studies.

Further efforts to categorize existing data for a series of related polymers will be made. Initially the categorization will consist of a manually tabulated series of facts; however, as these data are compiled, it is foreseeable that some form of computer analysis would be valuable.

REFERENCES

1. D. E. Gilmartin and C. A. Gaulin, A Quantitative Gas Calibration Technique for Mass Spectrometry, SAMSO-TR-75-20 (Space and Missile Systems Organization, Los Angeles, Calif., 7 January 1975).
2. G. A. Kleineberg, D. L. Geiger, and W. T. Gormley, *Die Makromolekular Chemie* 175 (2), 483 (1974).
3. R. H. Pritchard and I. J. Goldfarb, Computer Analysis of the Mass Spectra of Gas Mixtures, AFML-TR-73-280 (Air Force Materials Laboratory, Wright Patterson Air Force Base, Ohio, January 1975).
4. E. Stenhagen, S. Abrahamsson, and F. W. McLafferty, Atlas of Mass Spectral Data, Vols. 1, 2, and 3 (Interscience, New York, 1969).
5. F. P. Lossing, A. W. Tickner and W. A. Bryce, *J. Chem. Phys.* 19, 1254 (1951).
6. A. G. Harrison, E. G. Jones, S. K. Gupta, and G. P. Nagy, *Can. J. Chem.* 44, 1967 (1966).
7. J. A. Beran and L. Kevan, *J. Phys. Chem.* 73, 3866 (1969).